

NTIS BILL COPY

Polytechnic

UNIVERSITY

(1)

ANNUAL REPORT

TO

OFFICE OF NAVAL RESEARCH

UNDER

CONTRACT N00014-89-J-1512

FOR RESEARCH ON

ARRAY SIGNAL PROCESSING:
NEW TECHNIQUES FOR DIRECTION FINDING
AND SPECTRUM ESTIMATION

DTIC
S ELECT
OCT 20
E ce

DECLASSIFICATION STATEMENT A

Approved for public release
Distribution Unlimited

POLYTECHNIC UNIVERSITY

DEPARTMENT OF ELECTRICAL ENGINEERING AND COMPUTER SCIENCE

333 JAY STREET, BROOKLYN, NEW YORK 11201

AD-A213 883

83 10 24 137

ANNUAL REPORT

TO

OFFICE OF NAVAL RESEARCH

UNDER

CONTRACT N00014-89-J-1512

FOR RESEARCH ON

ARRAY SIGNAL PROCESSING:
NEW TECHNIQUES FOR DIRECTION FINDING
AND SPECTRUM ESTIMATION



Principal Investigator: **S. Unnikrishna Pillai**
Associate Professor
Department of Electrical Engineering &
Computer Science
Polytechnic University
333 Jay Street
Brooklyn, New York 11201

Contract Period: **January 1, 1989 - December 31, 1991**

Report Period: **January 1989 - October 1989**

Report Date: **October 1989**

Accession	
NTIS	CRA&I <input checked="" type="checkbox"/>
DTIC	TAB <input type="checkbox"/>
Unannounced <input type="checkbox"/>	
Justification	
By <i>per CG</i>	
Distribution	
Availability Codes	
Dist	Availability for Special
A-1	

Table of Contents

Description of work and FY88 progress	1
List of Publications under ONR contract in 1989	2
Technical Report	4
Appendix A:	
New Resolution Threshold Results in Three Source Scenes	5
Appendix B:	
A New Spectrum Extension Method That Maximizes The Two-Step Prediction Error - Generalization of Maximum Entropy Method	40

TITLE: Array Signal Processing: New Techniques for Direction Finding and Spectrum Estimation

PRINCIPAL INVESTIGATOR: Dr. S. Unnikrishna Pillai

LOCATION: Polytechnic University
Department of Electrical Engineering &
Computer Science
333 Jay Street
Brooklyn, New York 11201

TELEPHONE: (718) 260-3732

R & T #:

CONTRACT #: N00014-89-J-1512

SCIENTIFIC OFFICER: Dr. R. Madan

DESCRIPTION OF WORK: The objective of this contract is to develop new robust techniques for estimating the directions of arrival of multiple signals utilizing the available multi-sensor information. This includes direct procedures utilizing the generalized eigenvalues associated with certain matrices generated from the signal subspace eigenvectors of the actual array output matrix. In addition, this proposal addresses the problem of analyzing these techniques to evaluate their performance when the array output cross-covariances are directly estimated from the data. In this regard, the mean and variance expressions for the angle-of-arrival estimators can be used to derive thresholds for resolving two or more closely spaced sources.

Further, by interpreting the maximum entropy method (MEM) of spectrum estimation in terms of maximization of minimum mean square error for a one step predictor, a new class of spectrum extension problems to identify the best r-step predictors is proposed.

FY88 PROGRESS: A comprehensive asymptotic analysis of a class of high resolution estimators for resolving correlated and coherent sources in white noise has been completed. Using these results resolution thresholds have been derived in two and three source scenes for uncorrelated as well as coherent situations.

Given a finite set of n autocorrelations of a stationary discrete-time stochastic process, the well known problem of extending this given sequence so that the power spectral density associated with the resulting infinite sequence is nonnegative everywhere is further investigated. Motivated by the maximum entropy extension, which is equivalent to the maximization of the minimum mean square error (MMSE) associated with one-step predictors, the natural extension of maximizing the MMSE for r -step predictors compatible with the given correlations is studied. This analysis shows the resulting spectrum corresponds to that of a stable ARMA $(n, r - 1)$ process.

List of Publications under ONR contract in 1989

Papers submitted to Journals

1. D. Pearson, S. Unnikrishna Pillai, and Y. J. Lee, "An Algorithm for Near-Optimal Placement of Sensor Elements," submitted to *IEEE Transactions on Information Theory*.
2. S. Unnikrishna Pillai, Theodore I. Shim and Hamid Benteftifa, "A New Spectrum Extension Method that Maximizes the Two-Step Prediction Error—Generalization of Maximum Entropy Method," submitted to the *IEEE Transaction on Acoustics, Speech, and Signal Processing*

Book

3. S. Unnikrishna Pillai, *Array Signal Processing*, /221 pp/ Springer - Verlag, March 1989.

Journal Papers Published

4. S. Unnikrishna Pillai and B. H. Kwon, "Forward/Backward Spatial Smoothing Techniques for Coherent Signal Classification," *IEEE Transactions on Acoustics, Speech, and Signal Processing*, Vol. ASSP-37, No. 1, pp.8-15, January 1989.
5. ✓ S. Unnikrishna Pillai, and Y. J. Lee, "Coherent Signal Classification Using Symmetry Considerations," *IEEE Transactions on Acoustics, Speech, and Signal Processing*, Vol. ASSP-37, No. 1, pp. 135-138, January 1989.
6. ✓ Dante C. Youla and S. Unnikrishna Pillai, "A Uniqueness Characterization in Terms of Signed-Magnitude for Functions in the Polydisc Algebra $A(U^n)$," *Journal of Optical Society of America*, Vol. 6, No. 6, pp. 859-862, June 1989.
7. ✓ B. H. Kwon and S. Unnikrishna Pillai, "A Self Inversive Array Processing Scheme for Angle-of-Arrival Estimation," *European Signal Processing Journal*, Vol. 17, No. 3, pp. 259-277, July 1989.
8. ✓ S. Unnikrishna Pillai and B. H. Kwon, "Performance Analysis of MUSIC-Type High Resolution Estimators for Direction Finding in Correlated and Coherent Scenes," *IEEE Transactions on Acoustics, Speech, and Signal Processing*, Vol. ASSP-37, No. 8, pp. 1176-1189, August, 1989.

Conference Publications

9. B. H. Kwon and S. Unnikrishna Pillai, "Three Source Scenes--New Results on Signal Resolution," to be presented at the twenty third annual Asilomar Conference on Signals, Systems, and Computers, Pacific Grove, CA, October 30 - November 1, 1989.
10. S. Unnikrishna Pillai, "Signal Resolution Using Generalized Eigenvalues for Coherent Sources," to appear in the Proceedings of TENCON - 89, IEEE Region-10 Conference, Bombay, India, November 22-24, 1989.
11. S. Unnikrishna Pillai, "A New Spectrum Extension Method that Maximizes the Two Step Prediction Error," to appear in the Proceedings of Indo-US workshop on High Speed Digital processing, New Delhi, India, November 27-29, 1989.


Graduate Student(s) Supported

1. **Byung Ho Kwon**
Full time Ph.D. student and research fellow under this contract until May 1989. Completed his Ph.D. in February 1989.
Ph.D. dissertation title: "New High Resolution Techniques and Their Performance Analysis for Angles-of-Arrival Estimation."
2. **Theodore I. Shim**
Full time Ph.D. student and research fellow under this contract since January 1989.

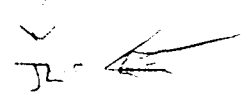
Electrical Engineering Seminars Delivered by the P. I.

1. "Some New Results on High Resolution Direction Finding," Moore School of Electrical Engineering, University of Pennsylvania, PA, March 30, 1989.
2. "Adaptive High Resolution Bearing Estimation," presented two lectures at the Tutorial workshop on *Applications of Adaptive Signal Processing in Radar*, Department of Electrical Engineering, National Taiwan University, Taipei, Taiwan, August 1-3, 1989.

Technical Report

 This research report concerns primarily with new algorithms in estimating signals from sensor output measurements. A complete performance analysis of the proposed algorithms is developed in Appendix A together with new results for resolving two and three uncorrelated/coherent signals.

Appendix B concerns with the problem of extending a given set of n autocorrelations so that the power spectral density associated with the resulting infinite sequence is nonnegative everywhere. Motivated by the maximum entropy method, which is equivalent to the maximization of the minimum mean square error (MMSE) associated with one-step predictors, the natural extension of maximizing the MMSE for r -step predictors compatible with the given correlations is studied. It is shown here for the first time that the resulting spectrum corresponds to that of a stable ARMA $(n, r - 1)$ process. The details of this optimum filter for a two step predictor are presented in Appendix B along with several other interesting conclusions.



Appendix A

New Resolution Threshold Results in Three Source Scenes

Abstract

This paper presents new performance analysis results in a three-source scene, when MUSIC-type high resolution estimators are used to estimate the directions of arrival of incoming signals. A two-source scenario has been popularly used to measure the quality of various estimators in terms of the SNR required to resolve (resolution threshold) two closely spaced sources. Similar results in a more realistic three-source scene is presented here for uncorrelated as well as coherent situations along with some interesting possibilities that deserve further study.

I. Introduction

Given a set of alternatives that perform identically under ideal conditions, one important question is how to measure their robustness or sensitiveness to imperfections that will invariably exist in reality. To illustrate this, consider the array processing scene where a set of sensors collect data from signals present in their field of view in presence of noise. Under the assumption that the sensor noise are independent and identical between themselves, a variety of high resolution techniques have been developed in the recent past [1 - 5] to estimate the directions of arrival of incoming signals. They all depend on the fact that the covariance matrix formed from the sensor array output data has several interesting structural properties. For example, in an equal noise situation when none of the signals present in the scene are completely coherent with each other, the direction vectors associated with the actual arrival angles can be shown to be orthogonal to the eigenvectors corresponding to the lowest eigenvalue of the array output covariance matrix. This forms the basis for the MUSIC

* The authors are with the department of Electrical Engineering and Computer Science at Polytechnic University, Brooklyn, New York. This work was supported by the Office of Naval Research under contract N-00014-89-J-1512.

algorithm [1] and several of its successors.

The coherent source situation can also be brought under this formulation, by employing certain preprocessing on sections of the array output covariance matrix. In this regard, the subarray averaging scheme [6-8] effectively creates a smoothed covariance matrix that is structurally identical to a covariance matrix in some correlated situation. Even more recent schemes such as ESPRIT, TLS-ESPRIT [3, 9], that make use of an underlying rotational invariance property of certain vectors in the signal subspace stems from the above idea. More interestingly, under ideal conditions, all these techniques perform identically, i.e., when the ensemble averages of the array output covariances are exactly known, any source situation that is resolvable by any one of these techniques can also be resolved by any other scheme that belongs to this general category, in contrast to - say - the linear prediction method.

However, the situation is entirely different when array output data is used to estimate these covariances. In that case, all these techniques can be viewed as distinct algorithms and they will perform differently for the same source scene. Several criteria have been proposed to evaluate their performance under such conditions. Of these the bias and variance of the estimator give reasonable information about the robustness of the estimator under consideration compared to other techniques. A more meaningful physical measure under these circumstances is the signal-to-noise ratio (SNR) required to resolve two closely spaced sources. At least qualitatively, this information tells about the sensitivity or superiority of the technique under consideration. The bias and variance expressions described above has been used in this connection to evaluate the resolution threshold in a variety of two source scenarios [10-13].

Naturally, two source scene is often unrealistic, and to evaluate the degradation in performance of these estimators in a general set up it is necessary to analyze at least a three-source scene. Reevaluating the resolution threshold in such a scene will also indicate the relative degradation in performance because of the presence of yet

another source and in this paper we propose to address this problem in uncorrelated and coherent situations.

II. Main Results in a Three-Source Scene

In this section we will consider three source scenarios in two extreme situations, viz, the uncorrelated case and the coherent case. The uncorrelated case represents the best possible scene in terms of the SNR required to resolve three signals and the coherent scene represents the worst scenario because of the complete dependence among the signals. As remarked earlier, the coherent scene can be decorrelated by employing the forward/backward smoothing scheme on the subarray output covariance matrices [8]. Though, in general, this requires additional number of sensor elements, interestingly any source scene containing two coherent signals can be decorrelated without the use of extra sensor elements. In fact, the mean of the array output covariance matrices corresponding to the forward array and its complex conjugated backward version can always resolve any such source scene [8] and for uniformity in comparison, we will adopt this situation in this study. Thus, the coherent scene under discussion here will consist of two coherent signals that are uncorrelated with the third signal. The analysis that follows in that case will utilize the forward/backward smoothing scheme that employs the forward array and its complex conjugated backward version to decorrelate and resolve the three signals and their arrival angles. To begin with, we consider the uncorrelated source scene.

II.A Uncorrelated Signals

Consider three uncorrelated, planar source waveforms $u_1(t)$, $u_2(t)$ and $u_3(t)$ arriving at an M -element uniform linear array along the directions θ_1 , θ_2 and θ_3 with respect to the line of the array. Under i.i.d. noise conditions the $M \times M$ array output covariance matrix has the form⁽¹⁾ [8]

$$\mathbf{R} = \mathbf{A} \mathbf{R}_u \mathbf{A}^\dagger + \sigma^2 \mathbf{I} \quad (1)$$

where the uncorrelated condition among the sources implies that, the source covariance matrix has the form $\mathbf{R}_u = \text{diag} [P_1, P_2, P_3]$ where $P_i \triangleq E[|u_i(t)|^2]$, $i = 1, 2, 3$ represents the signal power. Moreover

$$\mathbf{A} = \sqrt{M} [\mathbf{a}(\omega_1), \mathbf{a}(\omega_2), \mathbf{a}(\omega_3)] \quad (2)$$

where

$$\mathbf{a}(\omega_k) = \frac{1}{\sqrt{M}} [1, e^{-j\omega_k}, e^{-j2\omega_k}, \dots, e^{-j(M-1)\omega_k}]^T, \quad \omega_k \triangleq \pi \cos \theta_k \quad (3)$$

represents the direction vector associated with the arrival angle θ_k and $\sigma^2 = E[|n_i(t)|^2]$, $i = 1, 2, \dots, M$ denotes the common noise variance.

If $\lambda_1 \geq \lambda_2 \geq \dots \geq \lambda_M$ and $\beta_1, \beta_2, \dots, \beta_M$ represent the eigenvalues and corresponding normalized eigenvectors of \mathbf{R} , i.e.,

$$\mathbf{R} = \sum_{i=1}^M \lambda_i \beta_i \beta_i^\dagger \quad (4)$$

then in this particular setup $\lambda_i = \sigma^2$ for $i > 3$ and moreover $\beta_i^\dagger \mathbf{a}(\omega_k) = 0$, for all $i > 3$ and $k = 1, 2, 3$. Thus, the zeros of

$$Q(\omega) = \sum_{i=4}^M |\beta_i^\dagger \mathbf{a}(\omega)|^2 = 1 - \sum_{i=1}^3 |\beta_i^\dagger \mathbf{a}(\omega)|^2 \quad (5)$$

represents the true angles-of-arrival [1] and in principle, this estimator can resolve any three sources irrespective of their angular separation.

However, when array output data sample vectors are used in estimating \mathbf{R} by means of any standard procedure, the corresponding estimator in (5) is a random variable and the above conclusions are only approximately true. In fact, when the

(1) Hereonwards a (or A), a and A stand for scalar, vector and matrix in that order. Similarly, A^* , A^T and A^\dagger represent the complex conjugate, transpose and complex conjugate transpose of A respectively.

maximum likelihood method is used to estimate the covariance matrix \mathbf{R} using N data vectors, the associated estimates of eigenvectors so obtained can be used in (5) to generate the sample estimator $\hat{Q}(\omega)$. The statistical properties of $\hat{Q}(\omega)$ has been well documented in the case of zero mean complex circular Gaussian data for the general setup when smoothing is employed on the subarray covariance matrices to decorrelate coherent signals present in the data [11, 12]. As a special case of this general analysis, the bias and variance of the sample MUSIC estimator, $\hat{Q}(\omega)$ has been shown to be [11]

$$E[\hat{Q}(\omega)] = Q(\omega) + \frac{1}{N} \sum_{i=1}^K \frac{\lambda_i \sigma^2}{(\lambda_i - \sigma^2)^2} \left[(M - K) |\beta_i^\dagger \mathbf{a}(\omega)|^2 - Q(\omega) \right] + O\left(\frac{1}{N^2}\right) \quad (6)$$

and

$$Var(\hat{Q}(\omega)) = \frac{2}{N} Q(\omega) \sum_{i=1}^K \frac{\lambda_i \sigma^2}{(\lambda_i - \sigma^2)^2} |\beta_i^\dagger \mathbf{a}(\omega)|^2 + O\left(\frac{1}{N^2}\right). \quad (7)$$

Thus, in particular, within the above first-order approximation $Var(\hat{Q}(\omega_k)) \approx 0$, $1 \leq k \leq K$. However, along the true angles of arrival, $E[\hat{Q}(\omega_k)] \neq 0$ (see (6)) and the deviation of $E[\hat{Q}(\omega_k)]$ from zero - their nominal value - suggests the loss in resolution for this estimator below a certain angular separation. Since the estimator has zero variance along the true arrival angles, for a fixed number of samples a threshold in terms of SNR exists below which the nulls corresponding to the true arrival angles are no longer separately identifiable. Considering two sources at a time, the corresponding sources are separately identifiable if the bias at their middle angle is larger than the maximum of that at either of the two arrival angles. Letting $\theta_1 < \theta_2 < \theta_3$, this gives rise to the following inequalities for resolving three sources:

$$E[\hat{Q}((\omega_1 + \omega_2)/2)] \geq \max\{E[\hat{Q}(\omega_1)], E[\hat{Q}(\omega_2)]\} \quad (8)$$

and

$$E[\hat{Q}((\omega_2 + \omega_3)/2)] \geq \max \{E[\hat{Q}(\omega_2)], E[\hat{Q}(\omega_3)]\}. \quad (9)$$

When the sources are equispaced, i.e., $\omega_1 - \omega_2 = \omega_2 - \omega_3$, the minimum value of SNR that satisfies both (8) and (9) may be taken as the resolution threshold in a three-source scene. In the special case, when all signal powers are equal ($P_i = P, i = 1, 2, 3$), from the resulting symmetry it can be established that

$$E[\hat{Q}((\omega_1 + \omega_2)/2)] = E[\hat{Q}((\omega_2 + \omega_3)/2)],$$

$$E[\hat{Q}(\omega_2)] \geq E[\hat{Q}(\omega_1)] = E[\hat{Q}(\omega_3)]$$

and (8) and (9) collapses into

$$E[\hat{Q}((\omega_1 + \omega_2)/2)] \geq E[\hat{Q}(\omega_2)]. \quad (10)$$

Hence, by definition, the desired (normalized) resolution threshold $\xi \triangleq MP/\sigma^2$ satisfies (10) with an equality and in that case one can resolve three equipowered, uncorrelated sources.

To complete the analysis, from (6), it remains to obtain explicit expressions for the eigenvalues and eigenvectors associated with the signal subspace of \mathbf{R} and we proceed to do so in the next section.

II.B Eigenparameters in a Three Uncorrelated Source Scene

To begin with, notice that (from (1)) the three largest eigenvalues λ_1, λ_2 and λ_3 of \mathbf{R} are related to the eigenvalues μ_1, μ_2 and μ_3 of the 3×3 matrix, $\mathbf{R}_u \mathbf{A}^\dagger \mathbf{A}$ through the relation

$$\lambda_i = \mu_i + \sigma^2, \quad i = 1, 2, 3. \quad (11)$$

In an equipowered situation, however,

$$\mathbf{R}_u \mathbf{A}^\dagger \mathbf{A} = M P \begin{bmatrix} 1 & \rho_{12} & \rho_{13} \\ \rho_{12}^* & 1 & \rho_{23} \\ \rho_{13}^* & \rho_{23}^* & 1 \end{bmatrix} = M P \left(\mathbf{I}_3 + \begin{bmatrix} 0 & \rho_{12} & \rho_{13} \\ \rho_{12}^* & 0 & \rho_{23} \\ \rho_{13}^* & \rho_{23}^* & 0 \end{bmatrix} \right) \quad (12)$$

where

$$\rho_{ik} \triangleq \mathbf{a}^\dagger(\omega_i) \mathbf{a}(\omega_k) , \quad i, k = 1, 2, 3$$

represents the spatial correlation coefficient between the i^{th} and k^{th} sources. Thus, if ν_1, ν_2 and ν_3 represent the eigenvalues of the zero axial matrix

$$\mathbf{B} \triangleq \begin{bmatrix} 0 & \rho_{12} & \rho_{13} \\ \rho_{12}^* & 0 & \rho_{23} \\ \rho_{13}^* & \rho_{23}^* & 0 \end{bmatrix} , \quad (13)$$

then from (12)

$$\mu_i = M P (1 + \nu_i) , \quad i = 1, 2, 3. \quad (14)$$

Towards obtaining the eigenvalues of the above zero axial matrix, observe that in an equispaced source situation (i.e., $\omega_1 - \omega_2 = \omega_2 - \omega_3 \triangleq 2\omega_d$),

$$\rho_{12} = \rho_{23} = e^{j(M-1)\omega_d} \rho_s ; \quad \rho_s \triangleq \frac{\sin M \omega_d}{M \sin \omega_d} \quad (15)$$

and

$$\rho_{13} = e^{j 2(M-1)\omega_d} \frac{\sin 2M \omega_d}{M \sin 2\omega_d} = e^{j 2(M-1)\omega_d} \rho_s \rho_c ; \quad \rho_c \triangleq \frac{\cos M \omega_d}{\cos \omega_d} . \quad (16)$$

With (15) and (16) in (13), its eigenvalues satisfy the cubic equation

$$|\mathbf{B} - \nu \mathbf{I}_3| = \nu^3 - \rho_s^2 (2 + \rho_c^2) \nu - 2 \rho_s^3 \rho_c = 0. \quad (17)$$

Interestingly, the above equation can be factored into the form

$$(\nu + \rho_s \rho_c) (\nu^2 - \rho_s \rho_c \nu - 2 \rho_s^2)$$

and hence the three real roots of (17) are given by

$$\nu_2 = -\rho_s \rho_c$$

$$\nu_{1,3} = \frac{\rho_s}{2} \left(\rho_c \pm \sqrt{\rho_c^2 + 8} \right),$$

which gives the desired eigenvalues in (14) to be (in decreasing magnitude when ρ_s, ρ_c are positive; i.e., for small angular separations)

$$\mu_2 = M P (1 - \rho_s \rho_c) \quad (18.a)$$

$$\mu_1 = M P \left[1 + \frac{\rho_s}{2} \left(\rho_c + \sqrt{\rho_c^2 + 8} \right) \right] \quad (18.b)$$

$$\mu_3 = M P \left[1 + \frac{\rho_s}{2} \left(\rho_c - \sqrt{\rho_c^2 + 8} \right) \right] \quad (18.c)$$

From (4) and the discussion that follows, it is clear that the eigenvectors associated with (11) are linear combinations of the true direction vectors, i.e.,

$$\beta_i \propto a(\omega_1) + k_{1i} a(\omega_2) + k_{2i} a(\omega_3) \quad , \quad i = 1, 2, 3 \quad (19)$$

and

$$(\mathbf{A} \mathbf{R}_u \mathbf{A}^\dagger) \beta_i = M P \left[a(\omega_1) a^\dagger(\omega_1) + a(\omega_2) a^\dagger(\omega_2) + a(\omega_3) a^\dagger(\omega_3) \right] \beta_i = \mu_i \beta_i \quad i = 1, 2, 3. \quad (20)$$

With (19) in (20) and equating coefficients of the true direction vectors, we obtain three consistent equations for each i . Using two of these equations the unknowns k_{1i} and k_{2i} in (19) can be evaluated (for details, see section II.C) and after some algebra, this gives

$$\beta_2 \propto \left(e^{j(M-1)\omega_d} a(\omega_1) - e^{-j(M-1)\omega_d} a(\omega_3) \right)$$

$$\beta_1 \propto \left[1 + \frac{\rho_c^2}{2} + \frac{\rho_c \sqrt{\rho_c^2 + 8}}{2} \right] \left(e^{j(M-1)\omega_d} a(\omega_1) + e^{-j(M-1)\omega_d} a(\omega_3) \right) + \left[\frac{3\rho_c}{2} + \frac{\sqrt{\rho_c^2 + 8}}{2} \right] a(\omega_2)$$

and

$$\beta_3 \propto \left[1 + \frac{\rho_c^2}{2} - \frac{\rho_c \sqrt{\rho_c^2 + 8}}{2} \right] \left(e^{j(M-1)\omega_d} a(\omega_1) + e^{-j(M-1)\omega_d} a(\omega_3) \right) + \left[\frac{3\rho_c}{2} - \frac{\sqrt{\rho_c^2 + 8}}{2} \right] a(\omega_2).$$

Letting

$$\mathbf{u}_i = e^{j(M-1)\omega_i/2} \mathbf{a}(\omega_i) \quad i = 1, 2, 3 \quad (21)$$

and normalizing the above vectors, with the help of $\mathbf{u}_1^\dagger \mathbf{u}_2 = \mathbf{u}_2^\dagger \mathbf{u}_3 = \rho_s$, $\mathbf{u}_1^\dagger \mathbf{u}_3 = \rho_s \rho_c$, we obtain the desired eigenvectors to be

$$\beta_2 = \frac{\mathbf{u}_1 - \mathbf{u}_3}{\sqrt{2(1 - \rho_s \rho_c)}} \quad (22)$$

and

$$\beta_i = \frac{c_{1i}(\mathbf{u}_1 + \mathbf{u}_3) + c_{2i} \mathbf{u}_2}{\sqrt{2c_{1i}^2(1 + \rho_s \rho_c) + 4c_{1i}c_{2i}\rho_s + c_{2i}^2}} \quad i = 1, 3 \quad (23)$$

where

$$c_{1i} = 1 + \frac{\rho_c^2}{2} \pm \frac{\rho_c \sqrt{\rho_c^2 + 8}}{2} ; c_{2i} = \frac{3\rho_c}{2} \pm \frac{\sqrt{\rho_c^2 + 8}}{2} .$$

Notice that β_2 is orthogonal to \mathbf{u}_2 and is a linear combination of \mathbf{u}_1 and \mathbf{u}_3 only.

As remarked earlier, the desired resolution threshold satisfies (10) with an equality and in an equipowered, equispaced three source scene the above eigenparameters can be used to evaluate that explicitly. Towards this purpose using (11) and (14) we get

$$\frac{\lambda_i \sigma^2}{(\lambda_i - \sigma^2)^2} = \frac{(\mu_i + \sigma^2) \sigma^2}{\mu_i^2} = \frac{1}{\xi l_i} + \frac{1}{\xi^2 l_i^2} \quad (24.a)$$

where the array output signal-to-noise ratio is

$$\xi \triangleq M P / \sigma^2$$

and

$$l_i \triangleq 1 + \nu_i, \quad i = 1, 2, 3. \quad (24.b)$$

Thus with $K = 3$, from (6)

$$E[\hat{Q}(\omega_2)] = \frac{M-3}{N} \sum_{i=1}^3 \left[\frac{|\beta_i^\dagger \mathbf{a}(\omega_2)|^2}{\xi l_i} + \frac{|\beta_i^\dagger \mathbf{a}(\omega_2)|^2}{\xi^2 l_i^2} \right] + O\left(\frac{1}{N^2}\right) \quad (25)$$

and similarly with $\omega_m = (\omega_1 + \omega_2)/2$ representing the middle angle, we have

$$\begin{aligned} E[\hat{Q}(\omega_m)] = Q(\omega_m) + \frac{1}{N} \sum_{i=1}^3 \left[\frac{(M-3) |\beta_i^\dagger \mathbf{a}(\omega_m)|^2 - Q(\omega_m)}{\xi l_i} \right. \\ \left. + \frac{(M-3) |\beta_i^\dagger \mathbf{a}(\omega_m)|^2 - Q(\omega_m)}{\xi^2 l_i^2} \right] + O\left(\frac{1}{N^2}\right). \end{aligned} \quad (26)$$

Finally, equating (25) and (26) and neglecting terms of order less than $1/N$, we obtain the quadratic equation

$$a_3 \xi^2 + b_3 \xi + c_3 = 0 \quad (27)$$

and this gives the desired resolution threshold output SNR in an equipowered, equispaced, uncorrelated source scene to be

$$\xi_3 = \frac{-b_3 + \sqrt{b_3^2 - 4a_3c_3}}{2a_3}. \quad (28)$$

Here

$$\begin{aligned} a_3 &\triangleq Q(\omega_m) \\ b_3 &\triangleq \frac{1}{N} \sum_{i=1}^3 \frac{(M-3)(|\beta_i^\dagger \mathbf{a}(\omega_m)|^2 - |\beta_i^\dagger \mathbf{a}(\omega_2)|^2) - Q(\omega_m)}{l_i} \\ c_3 &\triangleq \frac{1}{N} \sum_{i=1}^3 \frac{(M-3)(|\beta_i^\dagger \mathbf{a}(\omega_m)|^2 - |\beta_i^\dagger \mathbf{a}(\omega_2)|^2) - Q(\omega_m)}{l_i^2} \end{aligned}$$

and $l_i, \beta_i, i = 1, 2, 3$ are as in (22)-(24).

The corresponding threshold results in a two source scene can be utilized to estimate the degradation in performance created by the presence of a third source. In the case of two equipowered uncorrelated sources, the resolution threshold has been shown to be [10],

$$\xi_2 = \frac{1}{N} \left\{ \frac{20(M-2)}{\Delta^4} \left[1 + \left[1 + \frac{N}{5(M-2)} \Delta^2 \right]^{1/2} \right] \right\} \quad (29)$$

where

$$\Delta^2 \triangleq M^2 \omega_d^2 / 3.$$

Though ξ_3 and ξ_2 possess similar features, for a given array the resolution threshold in the three source case can be much larger than that in the two source case. The above asymptotic analysis is also found to be in agreement with Monte Carlo simulation results. Table 1 represents a typical case study. Simulation results indicate that when equality holds in (10), the probability of resolution ranges between 33 to 50 percent in both cases. This suggests that the above results should give an approximate threshold in terms of ξ for 0.33 to 0.5 probability of resolution region and comparisons are carried out in Fig.1 using (28), (29) together with simulation results from Table 1 for this range of probability of resolution. Fig. 2 shows another comparison for a different array length. From these data it is also clear that, for the same SNR, sources that are located around the broad side of the array can be much closer than those arriving along the line of the array. Notice that in all these comparisons, the source locations have been chosen such that they are always well within the main beam of the array.

Interestingly, these results indicate that the presence of a third source, that is symmetrically located with respect to the center source, increases the SNR required to resolve the original two sources approximately by a factor of two (in dBs). This in turn speaks for the sensitivity of the MUSIC-type eigenstructure based algorithms.

In the next subsection we proceed to analyze the coherent case, where two of the three signals present in the scene are completely coherent with each other and the third signal is uncorrelated with these two signals.

II.C Two Coherent Signals (and an Uncorrelated Signal)

As remarked earlier, the coherent scene under discussion here consists of two coherent signals that are uncorrelated with the third signal. The coherent signals can be the outermost ones or the adjacent ones, and since only one of these situations is symmetric, these two cases have to be analyzed separately. Thus (a) $u_1(t)$ and $u_3(t)$ are coherent and $u_2(t)$ is uncorrelated (the symmetric case) or (b) $u_1(t)$ and $u_2(t)$ are coherent and $u_3(t)$ is uncorrelated with the other two signals. Of these two situations, we will only deal with the seemingly 'simpler' symmetric case, the details of which itself turn out to be quite involved.

To begin with, in the symmetric case, consider the perfectly coherent situation, i.e., $u_3(t) = u_1(t)$ and the mid-signal $u_2(t)$ is uncorrelated with the adjacent ones. By employing the covariance matrices corresponding to the forward array and its complex conjugated backward version, the above coherent situation can be decorrelated. In that case the smoothed covariance matrices associated with the mean of the above covariance matrix has the form [12]

$$\tilde{\mathbf{R}} = \frac{\mathbf{R}^f + \mathbf{R}^b}{2} = P \mathbf{A} \begin{bmatrix} 1 & 0 & \bar{\rho}_t \\ 0 & 1 & 0 \\ \bar{\rho}_t^* & 0 & 1 \end{bmatrix} \mathbf{A}^\dagger + \sigma^2 \mathbf{I} \quad (30)$$

where

$$\bar{\rho}_t \triangleq \frac{1 + e^{j(M-1)\omega_1} e^{-j(M-1)\omega_3}}{2} \quad (31)$$

represents the effective correlation coefficient due to f/b smoothing⁽²⁾. Here \mathbf{R}^f and \mathbf{R}^b stand for the forward and backward array output covariance matrices. Clearly, \mathbf{R}^f is the same as \mathbf{R} in (1) and with Φ as in (A.9)

$$\mathbf{R}^b = \mathbf{A} \Phi^{M-1} \mathbf{R}_u^* \Phi^{-(M-1)} \mathbf{A}^\dagger + \sigma^2 \mathbf{I}.$$

Using (2) and (31) in (30), we have

$$\begin{aligned} \bar{\mathbf{R}} &= M P \left\{ \mathbf{a}(\omega_1) \mathbf{a}^\dagger(\omega_1) + \bar{\rho}_t^* \mathbf{a}(\omega_3) \mathbf{a}^\dagger(\omega_1) + \bar{\rho}_t \mathbf{a}(\omega_1) \mathbf{a}^\dagger(\omega_3) + \mathbf{a}(\omega_3) \mathbf{a}^\dagger(\omega_3) + \mathbf{a}(\omega_2) \mathbf{a}^\dagger(\omega_2) \right\} + \sigma^2 \mathbf{I} \\ &= \frac{MP}{2} \left(\mathbf{b}_1 \mathbf{b}_1^\dagger + \mathbf{b}_2 \mathbf{b}_2^\dagger + \mathbf{b}_3 \mathbf{b}_3^\dagger \right) + \sigma^2 \mathbf{I} = \frac{MP}{2} \mathbf{B} \mathbf{B}^\dagger + \sigma^2 \mathbf{I} \end{aligned}$$

where

$$\mathbf{b}_1 \triangleq \mathbf{a}(\omega_1) + \mathbf{a}(\omega_3)$$

$$\mathbf{b}_2 \triangleq \sqrt{2} \mathbf{a}(\omega_2)$$

$$\mathbf{b}_3 \triangleq e^{j(M-1)\omega_1} \mathbf{a}(\omega_1) + e^{j(M-1)\omega_3} \mathbf{a}(\omega_3)$$

and

$$\mathbf{B} \triangleq [\mathbf{b}_1, \mathbf{b}_2, \mathbf{b}_3].$$

Since $\bar{\mathbf{R}} = \sum_{i=1}^M \bar{\lambda}_i \bar{\beta}_i \bar{\beta}_i^\dagger$ with $\bar{\lambda}_i = \sigma^2$ for $i > 3$, again, the signal subspace eigen-

values $\bar{\lambda}_1, \bar{\lambda}_2, \bar{\lambda}_3$ of $\bar{\mathbf{R}}$ are related to the three positive eigenvalues $\bar{\mu}_1, \bar{\mu}_2, \bar{\mu}_3$ of $\mathbf{B}^\dagger \mathbf{B}/2$ through the relation,

$$\bar{\lambda}_i = M P \bar{\mu}_i + \sigma^2, \quad i = 1, 2, 3. \quad (32)$$

However,

(2) Clearly, $|\bar{\rho}_t|$ should not be equal to 1, or the angular separation ($= 2\omega_d$) should not be in the neighborhood of $k\pi/(M-1)$, $k = 0, 1, 2, \dots$. However, in general $u_3(t) = \alpha u_1(t)$, where α represents the complex attenuation and in that case the above restriction does not hold.

$$\frac{1}{2} \mathbf{B}^\dagger \mathbf{B} = \begin{bmatrix} \bar{\rho}_{11} & \bar{\rho}_{12} & \bar{\rho}_{13} \\ \bar{\rho}_{12}^* & \bar{\rho}_{22} & \bar{\rho}_{23} \\ \bar{\rho}_{13}^* & \bar{\rho}_{23}^* & \bar{\rho}_{33} \end{bmatrix},$$

where by definition

$$\bar{\rho}_{ij} = \frac{1}{2} \mathbf{b}_i^\dagger \mathbf{b}_j,$$

and in particular with

$$\rho_t \triangleq \cos 2(M-1)\omega_d, \quad (33)$$

and ρ_s, ρ_c as defined before, it is easy to show that

$$\bar{\rho}_{11} = \bar{\rho}_{33} = 1 + \rho_s \rho_c \rho_t \quad (34.a)$$

$$\bar{\rho}_{22} = 1 \quad (34.b)$$

$$\bar{\rho}_{12} = \sqrt{2} \rho_s \cos(M-1)\omega_d \quad (34.c)$$

$$\bar{\rho}_{23} = e^{j(M-1)\omega_2} \bar{\rho}_{12} \quad (34.d)$$

$$\bar{\rho}_{13} = e^{j(M-1)\omega_2} (\rho_s \rho_c + \rho_t). \quad (34.e)$$

It now follows that the eigenvalues of $\mathbf{B}^\dagger \mathbf{B}/2$ can be written as

$$\bar{\mu}_i = \bar{\rho}_{11} - \bar{\nu}_i = (1 + \rho_s \rho_c \rho_t) - \bar{\nu}_i, \quad i = 1, 2, 3 \quad (35)$$

where $\bar{\nu}_i$ are given by the real roots of the cubic equation

$$\begin{vmatrix} \bar{\nu} & \bar{\rho}_{12} & \bar{\rho}_{13} \\ \bar{\rho}_{12}^* & \bar{\nu} - \rho_s \rho_c \rho_t & \bar{\rho}_{23} \\ \bar{\rho}_{13}^* & \bar{\rho}_{23}^* & \bar{\nu} \end{vmatrix} =$$

$$\bar{\nu}^3 - \rho_s \rho_c \rho_t (\bar{\nu}^2 - |\bar{\rho}_{13}|^2) - (2|\bar{\rho}_{12}|^2 + |\bar{\rho}_{13}|^2) \bar{\nu} + 2\text{Re}(\bar{\rho}_{12} \bar{\rho}_{13}^* \bar{\rho}_{23}) = 0. \quad (36)$$

With (34.a) - (34.e) in (36), it reduces to

$$\begin{aligned} & \bar{\nu}^3 - \rho_s \rho_c \rho_t \left[\bar{\nu}^2 - (\rho_s \rho_c + \rho_t)^2 \right] - \left[2\rho_s^2(1 + \rho_t) + (\rho_s \rho_c + \rho_t)^2 \right] \bar{\nu} + 2\rho_s^2(1 + \rho_t)(\rho_s \rho_c + \rho_t) \\ & = \left[\bar{\nu} - (\rho_s \rho_c + \rho_t) \right] \left[\bar{\nu}^2 + \left[(\rho_s \rho_c + \rho_t) - \rho_s \rho_c \rho_t \right] \bar{\nu} - 2\rho_s^2(1 + \rho_t) - \rho_s \rho_c \rho_t (\rho_s \rho_c + \rho_t) \right] = 0. \end{aligned}$$

Thus, the roots of the above equation are given by

$$\bar{\nu}_2 = \rho_s \rho_c + \rho_t \quad (37.a)$$

$$\bar{\nu}_{1,3} = -\frac{1}{2} \left[(\rho_s \rho_c + \rho_t - \rho_s \rho_c \rho_t) \pm \sqrt{D} \right] \quad (37.b)$$

where

$$D = (\rho_s \rho_c + \rho_t + \rho_s \rho_c \rho_t)^2 + 8\rho_s^2(1 + \rho_t). \quad (37.c)$$

Finally with (37.a) - (37.b) in (35) and (32), we get the desired signal subspace eigenvalues to be

$$\bar{\lambda}_2 = M P \bar{\mu}_2 + \sigma^2 = M P (1 - \rho_s \rho_c)(1 - \rho_t) + \sigma^2 \quad (38)$$

$$\bar{\lambda}_{1,3} = M P \bar{\mu}_{1,3} + \sigma^2 = \frac{M P}{2} \left[1 + (1 + \rho_s \rho_c)(1 + \rho_t) \pm \sqrt{D} \right] + \sigma^2 \quad (39)$$

with D as defined in (37.c).

Towards obtaining the eigenvectors $\tilde{\beta}_1, \tilde{\beta}_2, \tilde{\beta}_3$ associated with these eigenvalues, notice that once again they are linear combinations of the true direction vectors or equivalently those of $\mathbf{u}_1, \mathbf{u}_2, \mathbf{u}_3$ with \mathbf{u}_i as given by (21). Thus,

$$\tilde{\beta}_i \propto \mathbf{u}_1 + k_{2i} \mathbf{u}_2 + k_{3i} \mathbf{u}_3, \quad i = 1, 2, 3. \quad (40)$$

To make further progress, we rewrite the smoothed covariance matrix $\tilde{\mathbf{R}}$ also in terms of $\mathbf{u}_1, \mathbf{u}_2$ and \mathbf{u}_3 . Using (21) and (33) in (30), this gives

$$\bar{\mathbf{R}} = M P \left[(\mathbf{u}_1 + \rho_t \mathbf{u}_3) \mathbf{u}_1^\dagger + \mathbf{u}_2 \mathbf{u}_2^\dagger + (\rho_t \mathbf{u}_1 + \mathbf{u}_3) \mathbf{u}_3^\dagger \right] + \sigma^2 \mathbf{I}. \quad (41)$$

Since

$$\bar{\mathbf{R}} \bar{\beta}_i = \bar{\lambda}_i \bar{\beta}_i, \quad i = 1, 2, 3, \quad (42)$$

with (32) and (41) in (42), it reduces to

$$\left[(\mathbf{u}_1 + \rho_t \mathbf{u}_3) \mathbf{u}_1^\dagger + \mathbf{u}_2 \mathbf{u}_2^\dagger + (\rho_t \mathbf{u}_1 + \mathbf{u}_3) \mathbf{u}_3^\dagger \right] \bar{\beta}_i = \bar{\mu}_i \bar{\beta}_i, \quad i = 1, 2, 3.$$

Finally, using (40) and equating coefficients of \mathbf{u}_i on both sides of the above equation, we obtain

$$\begin{bmatrix} \rho_s(1+\rho_t) & \rho_s\rho_c + \rho_t \\ 1-\bar{\mu}_i & \rho_s \\ \rho_s(1+\rho_t) & 1+\rho_s\rho_c\rho_t - \bar{\mu}_i \end{bmatrix} \begin{bmatrix} k_{2i} \\ k_{3i} \end{bmatrix} = \begin{bmatrix} \bar{\mu}_i - (1 + \rho_s\rho_c\rho_t) \\ -\rho_s \\ -(\rho_s\rho_c + \rho_t) \end{bmatrix}. \quad (43)$$

For reasons that will become apparent soon, using the first and third row this gives

$$\begin{bmatrix} k_{2i} \\ k_{3i} \end{bmatrix} = \begin{bmatrix} \left[(\rho_s\rho_c + \rho_t)^2 - (1 + \rho_s\rho_c\rho_t - \bar{\mu}_i)^2 \right] / \Delta_i \\ 1 \end{bmatrix} \quad (44)$$

provided

$$\Delta_i = \rho_s(1 + \rho_t) \left[(1 - \rho_s\rho_c)(1 - \rho_t) - \bar{\mu}_i \right] \neq 0.$$

Since $\Delta_2 = 0$ and Δ_1 and Δ_3 are nonzero, using (40) and (44), the eigenvectors $\bar{\beta}_1$ and $\bar{\beta}_3$ can be expressed as

$$\bar{\beta}_i \propto \rho_s(1 + \rho_t) \left[(1 - \rho_s\rho_c)(1 - \rho_t) - \bar{\mu}_i \right] (\mathbf{u}_1 + \mathbf{u}_3)$$

$$\begin{aligned}
& - \left[(1 - \rho_s \rho_c)(1 - \rho_t) - \bar{\mu}_i \right] (1 + \rho_s \rho_c \rho_t - \bar{\mu}_i + \rho_s \rho_c + \rho_t) \mathbf{u}_2 \\
& \propto \rho_s (1 + \rho_t) (\mathbf{u}_1 + \mathbf{u}_3) + \left[\bar{\mu}_i - (1 + \rho_s \rho_c)(1 + \rho_t) \right] \mathbf{u}_2 \quad \text{for } i = 1, 3.
\end{aligned}$$

By making use of the exact expressions for $\bar{\mu}_{1,3}$ from (39) in the above expression, the corresponding normalized eigenvectors take the form

$$\tilde{\beta}_i = \frac{\rho_s (1 + \rho_t) (\mathbf{u}_1 + \mathbf{u}_3) + \bar{c}_i \mathbf{u}_2}{\|\tilde{\beta}_i\|} \quad (45)$$

where

$$\bar{c}_i = \frac{1}{2} \left(1 - (1 + \rho_s \rho_c)(1 + \rho_t) \pm \left[(1 - (1 + \rho_s \rho_c)(1 + \rho_t))^2 + 8\rho_s^2(1 + \rho_t) \right]^{1/2} \right) \quad (46.a)$$

and

$$\|\tilde{\beta}_i\| = 2\rho_s^2(1 + \rho_t)^2(1 + \rho_s \rho_c) + 4\rho_s^2(1 + \rho_t)\bar{c}_i + \bar{c}_i^2. \quad (46.b)$$

Next we turn our attention to evaluate $\tilde{\beta}_2$. Since the determinant corresponding to the first two equations in (43) is not zero, they can be utilized for this purpose. In that case, proceeding as before it is easy to show that

$$\tilde{\beta}_2 \propto k_1 \mathbf{u}_1 + k_2 \mathbf{u}_2 + k_3 \mathbf{u}_3$$

where

$$k_1 = \rho_s^2(1 + \rho_t) + (\bar{\mu}_2 - 1)(\rho_s \rho_c + \rho_t)$$

$$k_2 = \rho_s \left[\bar{\mu}_2 - (1 - \rho_t)(1 - \rho_s \rho_c) \right]$$

$$k_3 = (\bar{\mu}_2 - 1)^2 - \rho_s \rho_c \rho_t (\bar{\mu}_2 - 1) - \rho_s^2(1 + \rho_t).$$

By making use of (38), it follows that $k_2 = 0$ and $k_3 = -k_1$, which gives

$$\tilde{\beta}_2 \propto \mathbf{u}_1 - \mathbf{u}_3$$

or, finally

$$\tilde{\beta}_2 = \frac{u_1 - u_3}{\sqrt{2(1 - \rho_s \rho_c)}}. \quad (47)$$

Clearly (38) – (39) together with (45) – (47) completely characterizes the signal subspace eigenparameters in a three-source scene consisting of two symmetrically located coherent signals and a centrally located uncorrelated signal in terms of the input signal specifications and the array geometry.

The bias and variance expressions in the f/b case can be used to obtain the corresponding resolution threshold in this case. General expression for bias in the f/b case has been shown to be [11,12]

$$\begin{aligned} \bar{\eta}(\omega) = E[\hat{Q}(\omega)] - \bar{Q}(\omega) = & \frac{1}{N} \sum_{i=1}^3 \left[\sum_{\substack{k=1 \\ k \neq i}}^M \frac{\bar{\Gamma}_{k k i i}}{(\bar{\lambda}_i - \bar{\lambda}_k)^2} (|\tilde{\beta}_i^\dagger \mathbf{a}(\omega)|^2 - |\tilde{\beta}_k^\dagger \mathbf{a}(\omega)|^2) \right. \\ & \left. - \sum_{\substack{k=1 \\ k \neq i}}^M \sum_{\substack{l=1 \\ l \neq i \\ k \neq l}}^M \frac{\bar{\Gamma}_{k l i i}}{(\bar{\lambda}_i - \bar{\lambda}_k)(\bar{\lambda}_i - \bar{\lambda}_l)} \mathbf{a}^\dagger(\omega) \tilde{\beta}_k \tilde{\beta}_l^\dagger \mathbf{a}(\omega) \right] + O\left(\frac{1}{N^2}\right) \end{aligned} \quad (48)$$

and

$$\begin{aligned} Var(\hat{Q}(\omega)) = & \frac{2}{N} \sum_{i=1}^3 \sum_{\substack{j=1 \\ k \neq i \\ l \neq j}}^3 \sum_{k=1}^M \sum_{l=1}^M \\ & \frac{\text{Re} \left[(\bar{\Gamma}_{k l j i} \mathbf{a}^\dagger(\omega) \tilde{\beta}_j \tilde{\beta}_l^\dagger \mathbf{a}(\omega) + \bar{\Gamma}_{k j l i} \mathbf{a}^\dagger(\omega) \tilde{\beta}_l \tilde{\beta}_j^\dagger \mathbf{a}(\omega)) \mathbf{a}^\dagger(\omega) \tilde{\beta}_k \tilde{\beta}_i^\dagger \mathbf{a}(\omega) \right]}{(\bar{\lambda}_i - \bar{\lambda}_k)(\bar{\lambda}_j - \bar{\lambda}_l)} + O\left(\frac{1}{N^2}\right) \end{aligned} \quad (49)$$

where

$$\bar{Q}(\omega) = 1 - \sum_{i=1}^3 |\tilde{\beta}_i^\dagger \mathbf{a}(\omega)|^2,$$

$$\bar{\Gamma}_{iklj} = \frac{1}{4} \left(\bar{\beta}_i^\dagger \mathbf{R}^f \bar{\beta}_k \bar{\beta}_l^\dagger \mathbf{R}^f \bar{\beta}_j + \bar{\beta}_i^\dagger \mathbf{R}^b \bar{\beta}_k \bar{\beta}_l^\dagger \mathbf{R}^b \bar{\beta}_j + \bar{\beta}_i^\dagger \mathbf{R}^f \bar{\gamma}_l \bar{\gamma}_j^\dagger \mathbf{R}^b \bar{\beta}_k + \bar{\beta}_i^\dagger \mathbf{R}^b \bar{\gamma}_l \bar{\gamma}_j^\dagger \mathbf{R}^f \bar{\beta}_k \right) \quad (50)$$

and $\bar{\gamma}_i$ is the inverted $\bar{\beta}_i^*$ vector with $\bar{\gamma}_{i,m} = \bar{\beta}_{i,M-m+1}^*$. As shown in Appendix A, $\bar{\gamma}_i$, $i = 1, 2, \dots, M$ form a complete set of eigenvectors for $\bar{\mathbf{R}}$ and using this together with certain relations regarding equivalence of eigenvector sets of a matrix, for the above source scenario it is shown in Appendix B that

$$\bar{\eta}(\omega) = \frac{1}{N} \left[\sum_{i=1}^3 \frac{\bar{\lambda}_i \sigma^2}{2(\bar{\lambda}_i - \sigma^2)^2} \left((M-3) |\bar{\beta}_i^\dagger \mathbf{a}(\omega)|^2 - \bar{Q}(\omega) \right) + B(\omega) \right] + O\left(\frac{1}{N^2}\right) \quad (51)$$

and

$$\text{Var}(\hat{Q}(\omega)) = \frac{2\bar{Q}(\omega)}{N} \sum_{i=1}^3 \frac{\bar{\lambda}_i \sigma^2}{(\bar{\lambda}_i - \sigma^2)^2} |\bar{\beta}_i^\dagger \mathbf{a}(\omega)|^2 + O\left(\frac{1}{N^2}\right) \quad (52)$$

where

$$B(\omega) = \frac{4P^2 M^2 \sin^2 2(M-1)\omega_d}{(\bar{\lambda}_2 - \bar{\lambda}_1)(\bar{\lambda}_2 - \bar{\lambda}_3)} |\bar{\beta}_2^\dagger \mathbf{u}_1|^2 \text{Re} \left(\bar{\beta}_3^\dagger \mathbf{u}_1 \mathbf{u}_1^\dagger \bar{\beta}_1 \mathbf{a}^\dagger(\omega) \bar{\beta}_3 \bar{\beta}_1^\dagger \mathbf{a}(\omega) \right).$$

Notice that the additional term $B(\omega)$ in (51) is independent of the noise variance σ^2 .

Once again, following (24.a) we obtain

$$E[\hat{Q}(\omega_2)] = \frac{M-3}{2N} \sum_{i=1}^3 \left[\frac{|\bar{\beta}_i^\dagger \mathbf{a}(\omega_2)|^2}{\bar{\mu}_i \xi} + \frac{|\bar{\beta}_i^\dagger \mathbf{a}(\omega_2)|^2}{\bar{\mu}_i \xi^2} \right] + \frac{B(\omega_2)}{N} + O\left(\frac{1}{N^2}\right) \quad (53)$$

$$\begin{aligned} E[\hat{Q}(\omega_m)] &= \bar{Q}(\omega_m) + \frac{1}{2N} \sum_{i=1}^3 \left[\frac{(M-3) |\bar{\beta}_i^\dagger \mathbf{a}(\omega_m)|^2 - \bar{Q}(\omega_m)}{\bar{\mu}_i \xi} \right. \\ &\quad \left. + \frac{(M-3) |\bar{\beta}_i^\dagger \mathbf{a}(\omega_m)|^2 - \bar{Q}(\omega_m)}{\bar{\mu}_i \xi^2} \right] + \frac{B(\omega_m)}{N} + O\left(\frac{1}{N^2}\right). \end{aligned} \quad (54)$$

Finally, equating (53) and (54) and rearranging the terms, the resolution threshold associated with a three-source scene consisting of two symmetrically located coherent signals and an uncorrelated center signal satisfies the relation

$$\bar{a}_3 \xi^2 + \bar{b}_3 \xi + \bar{c}_3 = 0. \quad (55)$$

Here

$$\bar{a}_3 = \bar{Q}(\omega_m) + \frac{B(\omega_m) - B(\omega_2)}{N} \quad (56.a)$$

$$\bar{b}_3 = \frac{1}{2N} \sum_{i=1}^3 \frac{(M-3) \left(|\tilde{\beta}_i^\dagger \mathbf{a}(\omega_m)|^2 - |\tilde{\beta}_i^\dagger \mathbf{a}(\omega_2)|^2 \right) - \bar{Q}(\omega_m)}{\bar{\mu}_i} \quad (56.b)$$

$$\bar{c}_3 = \frac{1}{2N} \sum_{i=1}^3 \frac{(M-3) \left(|\tilde{\beta}_i^\dagger \mathbf{a}(\omega_m)|^2 - |\tilde{\beta}_i^\dagger \mathbf{a}(\omega_2)|^2 \right) - \bar{Q}(\omega_m)}{\bar{\mu}_i^2}. \quad (56.c)$$

The signal subspace eigenparameters that have been obtained in (38) – (39) and (45) – (47) can be used to compute the desired resolution threshold in this case exactly. Once again the corresponding threshold expression in a two-coherent source scene can be utilized to estimate the degradation in performance by the presence of an uncorrelated, third center signal. In the case of two coherent sources, the resolution threshold has been shown to be [11]

$$\xi_2 = \frac{1}{N} \left[\frac{20(M-2)}{\Delta^4} \left(\frac{1}{3\Delta^2} - \frac{1}{20} - \frac{\Delta^2}{16} \right) \left(1 + \left(1 + \frac{N(M-2)}{5M(M-4)} \right)^2 \right) \right]. \quad (57)$$

Table 2 represents a typical case study for a three-source symmetric coherent scene described above. From these simulation results, equality between (53) and (54) corresponds to 0.33 to 0.5 probability of resolution and Fig. 3 shows comparisons between (55) and (57) for this probability of resolution.

Equation (55) is derived based on the assumption that inequalities in (8) – (10) are satisfied. However, in the coherent case for certain angular separations, the above inequalities can reverse their signs and in that case the above threshold expression is meaningless. This is because the relative magnitudes of eigenvalues can be different depending upon the actual angular separation and consequently the additional term $B(\omega)$ in the general bias expression in (51) can change its sign so as to reverse the inequalities in (8) – (10). Since $B(\omega)$ is independent of N and σ^2 , from (56.a), for large N , $\bar{a}_3 \approx \bar{Q}(\omega_m) > 0$ and in that case a solution always exists.

III. Conclusions

A three-source scene, under uncorrelated and coherent situations, is separately analyzed to evaluate the sensitivity and robustness of MUSIC-type high resolution estimators in resolving closely spaced sources. When the null spectrum estimator is used to locate the directions-of-arrival of incoming signals, for a fixed number of samples, a threshold in terms of SNR exists below which the nulls corresponding to the true arrival angles are no longer separately identifiable. Clearly, in a two-source scene the corresponding sources are separately identifiable if the bias at their middle angle is larger than the maximum of that at either of the two arrival angles. This definition is extended to three-source scenes here, by considering pairs of signals at a time and choosing the maximum of the respective threshold values to be the desired SNR required to resolve the three source situation. This is made possible by first obtaining parametric expressions for the eigenparameters in three source scenarios and using them in the appropriate bias expressions. The parametric expressions for eigenparameters in a three-uncorrelated and coherent situations (the two outermost signals are perfectly coherent and the center signal is uncorrelated with the coherent group) derived here is believed to be new.

The threshold SNR in three source scenes so obtained are compared with corresponding results in two source situations. These results indicate that in the

uncorrelated case, the presence of a third source increases the SNR required to resolve the original two sources approximately by a factor of two. It may be remarked that the smaller increment in SNR in the 'symmetric' coherent case can be attributed to the larger angular separation ($4\omega_d$ instead of $2\omega_d$) between the coherent signals in the three source case. In turn, these results also speak for the sensitivity of MUSIC-type eigenstructure based algorithms when an extra source is introduced into the scene.

In this paper we have only analyzed the symmetric coherent case. The other possibility, where an uncorrelated signal is introduced into a two coherent signal scene such that the angular separation between the uncorrelated and any one of the coherent signal is the same as that between the coherent signals deserves further study. This 'more natural' case seems to be quite involved because of the absence of any symmetry that is present in the coherent case analyzed in this paper.

References

- [1] R. O. Schmidt, "Multiple emitter location and signal parameter estimation," in *Proc. RADC Spectral Est. Workshop*, 1979, pp. 243-258. Also, "A signal subspace approach to multiple emitter location and spectral estimation", Ph.D dissertation, Stanford University, 1981.
- [2] G. Bienvenu, "Influence of the spatial coherence of the background noise on high resolution passive methods," in *Proc. IEEE ICASSP-79*, Washington, DC, 1979, pp. 306-309.
- [3] A. Paulraj, R. Roy, and T. Kailath, "Estimation of signal parameters via rotational invariance techniques - ESPRIT," in *Proc. 19th Asilomar Conf.*, Pacific Grove, CA, Nov. 1985.
- [4] R. Kumaresan and D. W. Tufts, "Estimation the angles of arrival of multiple plane waves," *IEEE Trans. Aerosp. Electron. Syst.*, vol. AES-19, Jan. 1983

- [5] H. Wang and M. Kaveh, "Coherent signal-subspace processing for the detection and estimation of angles of arrival of multiple wide-band sources," *IEEE Trans. Acoust., Speech, Signal Processing*, vol. ASSP-33, no. 4, pp. 823-831, Aug. 1985.
- [6] J. E. Evans, J. R. Johnson, and D. F. Sun, "Application of advanced signal processing techniques to angle of arrival estimation in ATC navigation and surveillance system," *M.I.T. Lincoln Lab.*, Lexington, MA, Rep. 582, 1982.
- [7] T. J. Shan, M. Wax, and T. Kailath, "On spatial smoothing for estimation of coherent signals," *IEEE Trans. Acoust., Speech, Signal Processing*, vol. ASSP-33, no. 4, pp. 806-811, Aug. 1985.
- [8] S. U. Pillai and B. H. Kwon, "Forward/backward spatial smoothing techniques for coherent signal identification," *IEEE Trans. Acoust., Speech, Signal Processing*, vol. ASSP-37, no. 1, pp. 8-15, Jan. 1989.
- [9] R. Roy and T. Kailath, "ESPRIT and total least square," in *Proc. 21th Asilomar Conf.*, Nov. 2-4, 1987.
- [10] M. Kaveh, and A. J. Barabell, "The statistical performance of the MUSIC and the minimum-norm algorithms in resolving plane waves in noise," *IEEE Trans. Acoust., Speech, Signal Processing*, vol. ASSP-34, no. 2, pp. 331-341, Apr. 1986.
- [11] S. U. Pillai, and B. H. Kwon, "Performance analysis of MUSIC-type high resolution estimators for direction finding in correlated and coherent scenes," to appear in *IEEE Trans. Acoust., Speech, Signal Processing*, vol. ASSP-37, no.8, Aug. 1989.
- [12] S. U. Pillai, *Array signal processing*, Springer-Verlag, New York, 1989.
- [13] B. H. Kwon, "New high resolution techniques and their performance analysis for angles-of-arrival estimation," Ph.D dissertation, Polytechnic University, June 1989.

Table 1

Resolution threshold and probability of resolution vs. angular separation for equipowered sources in an uncorrelated scene. (number of sensors = 7, number of snapshots = 100, number of simulations = 100). Probability of Resolution \triangleq Total number of successes in 100 simulations/100.

Angles of arrival			Angular Separation $2\omega_d$	Three source scene		Two source scene*	
θ_1	θ_2	θ_3		SNR(dB)	Prob	SNR(dB)	Prob.
34°	40°	45.33°	0.1979	23	0.26	9	0.28
				24	0.37	10	0.36
				25	0.43	11	0.47
				26	0.51	12	0.60
60°	66°	71.73°	0.2930	14	0.27	3	0.31
				15	0.33	4	0.36
				16	0.43	5	0.48
				17	0.53	6	0.61
127°	135°	144.33°	0.3308	11	0.23	2	0.27
				12	0.30	3	0.41
				13	0.41	4	0.53
				14	0.50		

* In the case of two source scene, the first two angles of arrival are used in actual simulation.

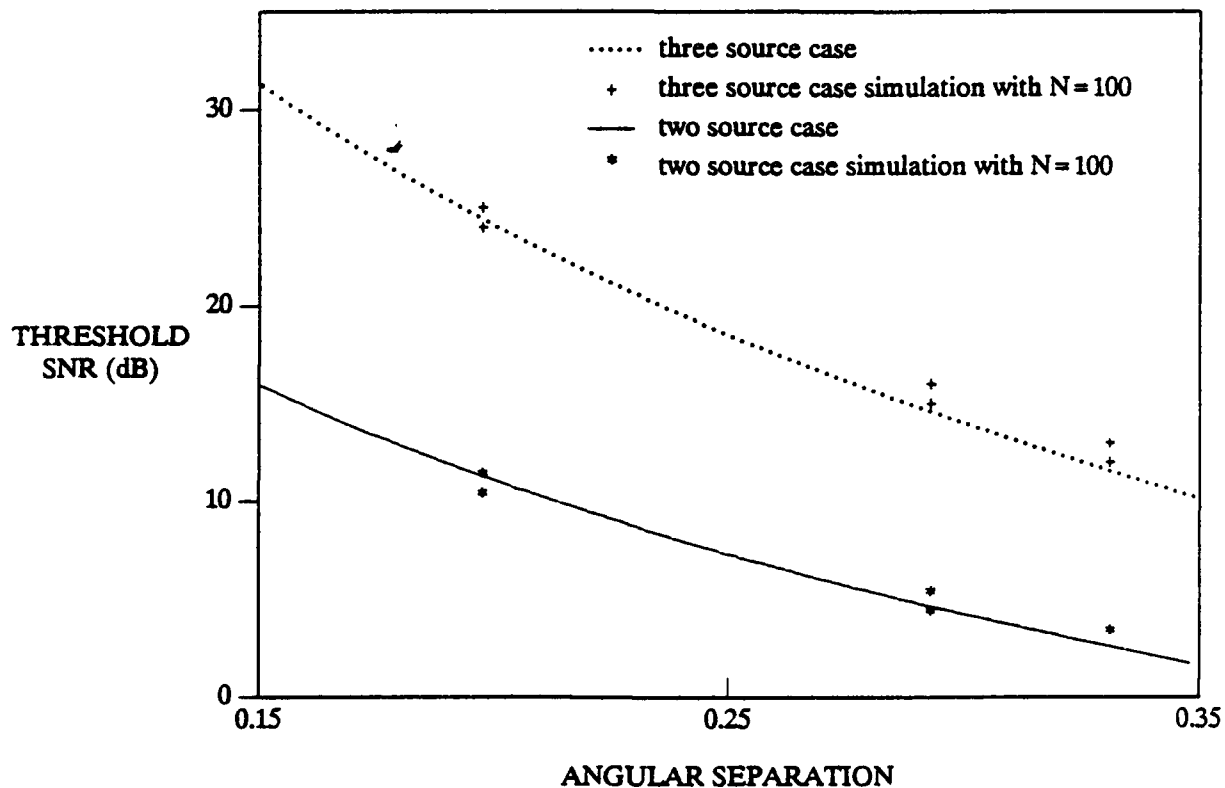


Fig. 1. Uncorrelated source scene: Resolution threshold vs angular separation for three equipowered signals as well as two equipowered signals. A seven element array is used to receive the signals in both cases. Each simulation point represents one hundred trials with probability of success for resolution ranging from 0.33 to 0.5.

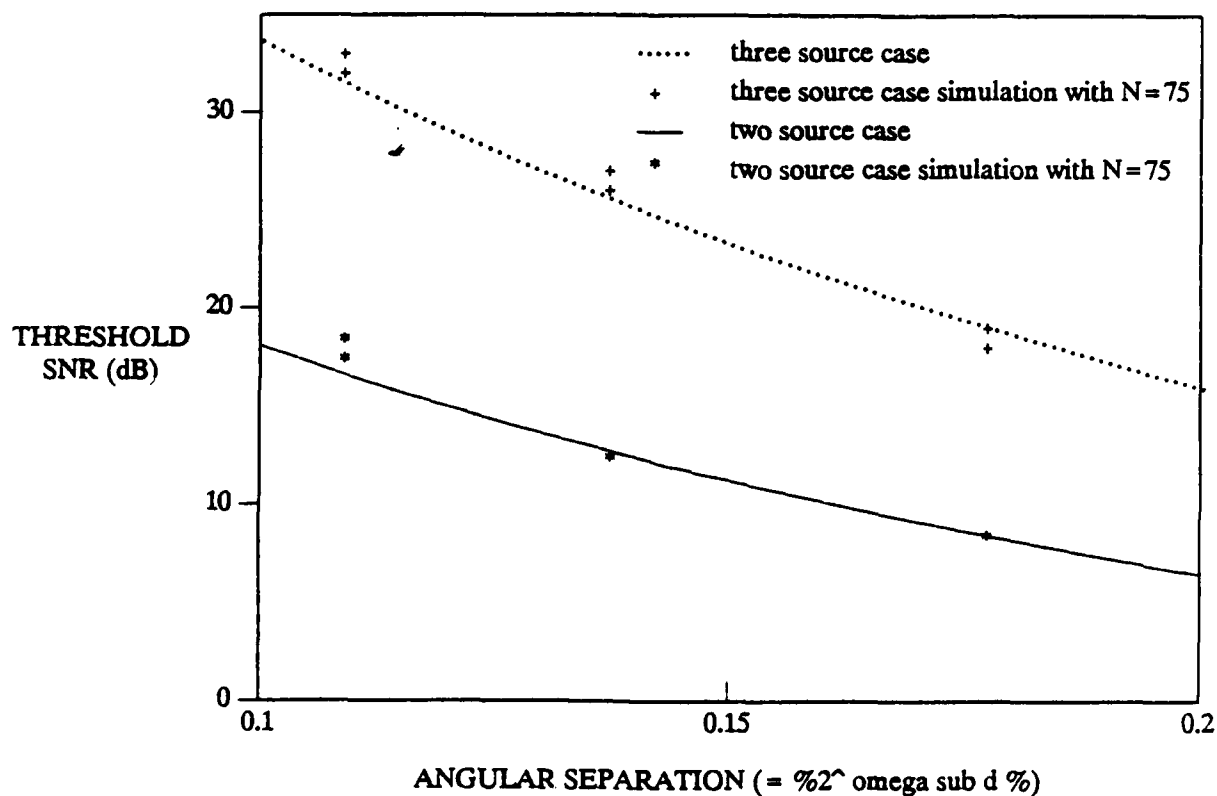


Fig. 2. Uncorrelated source scene: Resolution threshold vs angular separation for three equipowered signals as well as two equipowered signals. A ten element array is used to receive the signals in both cases. Each simulation point represents one hundred trials with probability of success for resolution ranging from 0.33 to 0.5.

Table 2

Resolution threshold and probability of resolution vs. angular separation for equipowered sources in a symmetric coherent scene. (number of sensors = 15, number of snapshots = 100, number of simulations = 100). Probability of Resolution \triangleq Total number of successes in 100 simulations/100.

Angles of arrival			Angular separation	Three source scene		Two source scene*	
θ_1	θ_2	θ_3	$2\omega_d$	SNR(dB)	Prob.	SNR(dB)	Prob.
155°	158°	161.45°	0.0656	28 29 30 31	0.31 0.34 0.41 0.54	23 24 25	0.17 0.35 0.67
110°	112°	114.03°	0.1024	19 20 21 22	0.27 0.37 0.48 0.64	12 13 14	0.16 0.36 0.59
55°	58°	60.90°	0.1372	12 13 14 15	0.25 0.37 0.47 0.61	4 5 6	0.23 0.38 0.63

* In the case of two source scene, the first two angles of arrival are used in actual simulation.

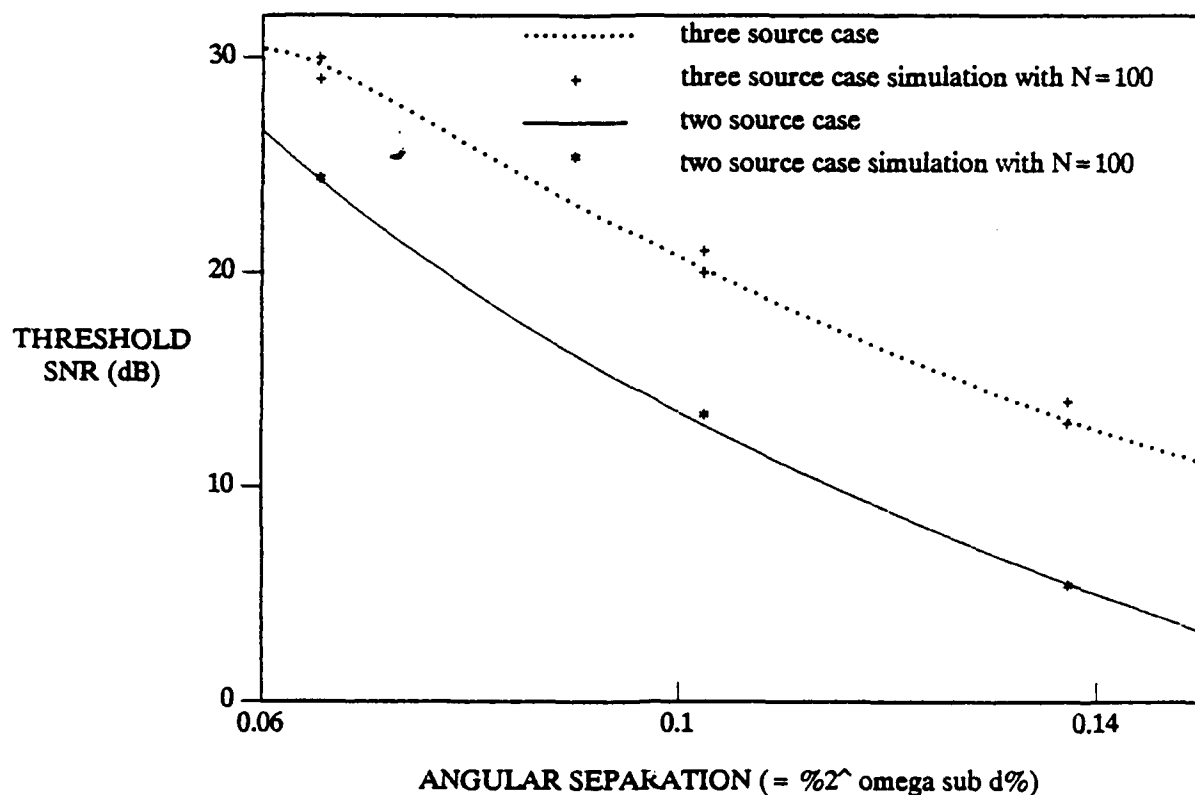


Fig. 3. Coherent source scene: Resolution threshold vs angular separation for three equipowered symmetric (two coherent and one uncorrelated) signals as well as two equipowered signals. A fifteen element array is used to receive the signals in both cases. Each simulation point represents one hundred trials with probability of success for resolution ranging from 0.33 to 0.5.

Appendix A

Consider an uncorrelated-source scene where at most two signals may be completely coherent. Thus either all signals are uncorrelated with each other or two are perfectly coherent, while the rest is uncorrelated with each other and with the coherent group. In both situations we will show that in the case of a uniform array, if $\tilde{\beta}_1, \tilde{\beta}_2, \dots, \tilde{\beta}_M$ denotes one set of eigenvectors of the smoothed covariance matrix $\tilde{\mathbf{R}}$, then their inverted and complex conjugated counterparts $\tilde{\gamma}_i = \mathbf{J} \tilde{\beta}_i^*, i = 1, 2, \dots, M$ also form a new set of eigenvectors of $\tilde{\mathbf{R}}$. Here by definition

$$\mathbf{J} = \begin{bmatrix} 0 & & 1 \\ & \ddots & \\ 1 & & 0 \end{bmatrix}.$$

Proof

Let

$$\tilde{\mathbf{B}} = [\tilde{\beta}_1, \tilde{\beta}_2, \dots, \tilde{\beta}_M] \quad (\text{A.1})$$

$$\tilde{\mathbf{G}} = [\tilde{\gamma}_1, \tilde{\gamma}_2, \dots, \tilde{\gamma}_M] = \mathbf{J} \tilde{\mathbf{B}}^*. \quad (\text{A.2})$$

The smoothed covariance matrix has the form

$$\tilde{\mathbf{R}} = \mathbf{A} \tilde{\mathbf{R}}_u \mathbf{A}^\dagger + \sigma^2 \mathbf{I} \quad (\text{A.3})$$

where

$$\mathbf{A} = \begin{bmatrix} 1 & 1 & \dots & 1 \\ \delta_1 & \delta_2 & \dots & \delta_K \\ \delta_1^2 & \delta_2^2 & \dots & \delta_K^2 \\ \vdots & \vdots & \ddots & \vdots \\ \delta_1^{M-1} & \delta_2^{M-1} & \dots & \delta_K^{M-1} \end{bmatrix} \quad (\text{A.4})$$

with $\delta_k = e^{-j\pi\omega_k}$, $k = 1, 2, \dots, K$ and $\tilde{\mathbf{R}}_u$ represents the smoothed source covariance matrix. Clearly, in the uncorrelated case

$$\tilde{\mathbf{R}}_u = \text{diag} [P_1, P_2, \dots, P_K] \quad (\text{A.5})$$

and in the latter case consisting of two coherent and uncorrelated signals - say - (the first and the second)

$$\tilde{\mathbf{R}}_u = \begin{bmatrix} P_1 & \rho_t & 0 & 0 & 0 \\ \rho_t^* & P_2 & 0 & 0 & 0 \\ 0 & 0 & P_3 & 0 & 0 \\ 0 & 0 & 0 & \cdot & 0 \\ 0 & 0 & 0 & 0 & P_K \end{bmatrix} \quad (\text{A.6})$$

where

$$\rho_t = \sqrt{P_1 P_2} \left(\frac{1 + \delta_1^{-(M-1)} \delta_2^{M-1}}{2} \right).$$

Since $\tilde{\beta}_i$, $1 \leq i \leq M$ represents a set of eigenvectors for $\tilde{\mathbf{R}}$, we have

$$\tilde{\mathbf{R}} = \tilde{\mathbf{B}} \mathbf{\Lambda} \tilde{\mathbf{B}}^\dagger \quad (\text{A.7})$$

where $\mathbf{\Lambda}$ is real, positive and diagonal. Now

$$\tilde{\mathbf{G}} \mathbf{\Lambda} \tilde{\mathbf{G}}^\dagger = \mathbf{J} \tilde{\mathbf{B}}^* \mathbf{\Lambda} (\mathbf{J} \tilde{\mathbf{B}}^*)^\dagger = \mathbf{J} \tilde{\mathbf{R}}^* \mathbf{J} = (\mathbf{J} \mathbf{A}^*) \tilde{\mathbf{R}}_u^* (\mathbf{J} \mathbf{A}^*)^\dagger + \sigma^2 \mathbf{I}. \quad (\text{A.8})$$

However, using (A.4)

$$\mathbf{J} \mathbf{A}^* = \mathbf{A} \Phi^{M-1}$$

where

$$\Phi = \text{diag} [\delta_1^{-1}, \delta_2^{-1}, \dots, \delta_K^{-1}] \quad (\text{A.9})$$

and hence (A.8) simplifies into

$$\begin{aligned}\tilde{G} \Lambda \tilde{G}^\dagger &= A (\Phi^{M-1} \tilde{R}_u^* \Phi^{-(M-1)}) A^\dagger + \sigma^2 I \\ &= A \tilde{R}_u A^\dagger + \sigma^2 I = \tilde{R}\end{aligned}\quad (A.10)$$

since $\Phi^{M-1} \tilde{R}_u^* \Phi^{-(M-1)} = \tilde{R}_u$ for either forms of \tilde{R}_u given by (A.5) or (A.6).

Interestingly, if some of the entries in Λ are distinct, say the first K , then since

$$\tilde{R} = \tilde{G} \Lambda \tilde{G}^\dagger = \tilde{B} \Lambda \tilde{B}^\dagger \quad (A.11)$$

with $V = \tilde{B}^\dagger \tilde{G}$, we have

$$V \Lambda = \Lambda V$$

or

$$\tilde{\lambda}_i v_{ij} = \tilde{\lambda}_j v_{ij}.$$

Since V is unitary this simplifies into

$$\tilde{\gamma}_i = \tilde{\beta}_i e^{j\phi_i}, \quad i = 1, 2, \dots, K \quad (A.12)$$

and

$$[\tilde{\gamma}_{K+1}, \tilde{\gamma}_{K+2}, \dots, \tilde{\gamma}_M] = [\tilde{\beta}_{K+1}, \tilde{\beta}_{K+2}, \dots, \tilde{\beta}_M] V_1 \quad (A.13)$$

where V_1 is an $(M-K) \times (M-K)$ unitary matrix.

Appendix B

In this Appendix, we evaluate the bias expression for symmetric coherent signal scene described in II.C. For $K = 3$, the first term of the general bias expression in (48) can be written as

$$\begin{aligned} \bar{\eta}_1 = \sum_{i=1}^3 \left[\sum_{\substack{k=1 \\ k \neq i}}^3 \frac{\bar{\Gamma}_{k k i i}}{(\bar{\lambda}_i - \bar{\lambda}_k)^2} \left(|\bar{\beta}_i^\dagger \mathbf{a}(\omega)|^2 - |\bar{\beta}_k^\dagger \mathbf{a}(\omega)|^2 \right) \right. \\ \left. + \sum_{k=4}^M \frac{\bar{\Gamma}_{k k i i}}{(\bar{\lambda}_i - \bar{\lambda}_k)^2} \left(|\bar{\beta}_i^\dagger \mathbf{a}(\omega)|^2 - |\bar{\beta}_k^\dagger \mathbf{a}(\omega)|^2 \right) \right]. \end{aligned} \quad (\text{B.1})$$

Then, by using (A.12), for $i, k \leq 3$ in (50) we have $\bar{\Gamma}_{k k i i} = \bar{\Gamma}_{i i k k}$ and for $i \leq 3$ and $k \geq 4$

$$4\bar{\Gamma}_{k k i i} = \sigma^2 \left(\bar{\beta}_i^\dagger \mathbf{R}^f \bar{\beta}_i + \bar{\beta}_i^\dagger \mathbf{R}^b \bar{\beta}_i \right) = 2\sigma^2 \bar{\lambda}_i.$$

With these identities, the first term in (B.1) can be shown to be zero and the second term can be expressed as

$$\bar{\eta}_1 = \sum_{i=1}^3 \frac{\bar{\lambda}_i \sigma^2}{2(\bar{\lambda}_i - \sigma^2)^2} \left((M - 3) |\bar{\beta}_i^\dagger \mathbf{a}(\omega)|^2 - \bar{Q}(\omega) \right). \quad (\text{B.2})$$

Now, consider the second term of (48) by partitioning it as

$$\begin{aligned} \bar{\eta}_2 \triangleq B(\omega) = \sum_{i=1}^3 \left[\sum_{\substack{k=1 \\ k \neq i}}^3 \sum_{\substack{l=1 \\ l \neq i}}^3 \frac{\bar{\Gamma}_{k l i i}}{(\bar{\lambda}_i - \bar{\lambda}_k)(\bar{\lambda}_i - \bar{\lambda}_l)} \mathbf{a}^\dagger(\omega) \bar{\beta}_k \bar{\beta}_l^\dagger \mathbf{a}(\omega) \right. \\ \left. + \sum_{\substack{k=1 \\ k \neq i}}^3 \sum_{l=4}^M \frac{\bar{\Gamma}_{k l i i}}{(\bar{\lambda}_i - \bar{\lambda}_k)(\bar{\lambda}_i - \bar{\lambda}_l)} \mathbf{a}^\dagger(\omega) \bar{\beta}_k \bar{\beta}_l^\dagger \mathbf{a}(\omega) + \sum_{k=4}^M \sum_{\substack{l=1 \\ l \neq i}}^3 \frac{\bar{\Gamma}_{k l i i}}{(\bar{\lambda}_i - \bar{\lambda}_k)(\bar{\lambda}_i - \bar{\lambda}_l)} \mathbf{a}^\dagger(\omega) \bar{\beta}_k \bar{\beta}_l^\dagger \mathbf{a}(\omega) \right] \end{aligned}$$

$$+ \sum_{\substack{k=4 \\ k \neq l}}^M \sum_{l=4}^M \frac{\bar{\Gamma}_{klil}}{(\bar{\lambda}_i - \bar{\lambda}_k)(\bar{\lambda}_i - \bar{\lambda}_l)} \mathbf{a}^\dagger(\omega) \tilde{\beta}_k \tilde{\beta}_l^\dagger \mathbf{a}(\omega) \Bigg] \quad (\text{B.3})$$

By applying the orthogonality property between $\tilde{\beta}_k$, $4 \leq k \leq M$ and $\mathbf{a}(\omega_i)$, $1 \leq i \leq 3$ in (50) and with the help of (A.11) – (A.12), it is easy to show that the last three terms of (B.3) are zeros. Also, from the structural properties of \mathbf{R}^f and \mathbf{R}^b , we obtain

$$\mathbf{R}^b = \mathbf{R}^f + j 2 P M \sin 2(M-1)\omega_d (\mathbf{u}_1 \mathbf{u}_3^\dagger - \mathbf{u}_3 \mathbf{u}_1^\dagger). \quad (\text{B.4})$$

Using this together with (50), we can evaluate the first term of (B.3). For $i, k, l \leq 3$ (i, k, l are all distinct),

$$\begin{aligned} 4\bar{\Gamma}_{klil} &= \tilde{\beta}_k^\dagger \mathbf{R}^f \tilde{\beta}_l \tilde{\beta}_i^\dagger \mathbf{R}^f \tilde{\beta}_i + \tilde{\beta}_k^\dagger \mathbf{R}^b \tilde{\beta}_l \tilde{\beta}_i^\dagger \mathbf{R}^b \tilde{\beta}_i - 2\tilde{\beta}_k^\dagger \mathbf{R}^f \tilde{\beta}_i \tilde{\beta}_i^\dagger \mathbf{R}^f \tilde{\beta}_l \\ &= j 2 P M \sin 2(M-1)\omega_d \left[\tilde{\beta}_k^\dagger \mathbf{R}^b \tilde{\beta}_l \tilde{\beta}_i^\dagger (\mathbf{u}_1 \mathbf{u}_3^\dagger - \mathbf{u}_3 \mathbf{u}_1^\dagger) \tilde{\beta}_i \right] - 2\tilde{\beta}_k^\dagger \mathbf{R}^f \tilde{\beta}_i \tilde{\beta}_i^\dagger \mathbf{R}^f \tilde{\beta}_l. \end{aligned} \quad (\text{B.5})$$

Here we have made use of the fact that $\tilde{\gamma}_i = \tilde{\beta}_i e^{j\phi_i}$ and

$$\tilde{\beta}_i^\dagger \mathbf{R}^b \tilde{\beta}_l = 2\bar{\lambda}_i \delta_{il} - \tilde{\beta}_i^\dagger \mathbf{R}^f \tilde{\beta}_l = -\tilde{\beta}_i^\dagger \mathbf{R}^f \tilde{\beta}_l \quad \text{for } i \neq l.$$

Making use of the explicit forms of $\tilde{\beta}_i$, $i = 1, 2, 3$ in (45) and (47), it can be shown that

$$\tilde{\beta}_i^\dagger (\mathbf{u}_1 \mathbf{u}_3^\dagger - \mathbf{u}_3 \mathbf{u}_1^\dagger) \tilde{\beta}_i = 0, \quad i = 1, 2, 3 \quad (\text{B.6})$$

and

$$\tilde{\beta}_1 \mathbf{R}^f \tilde{\beta}_3 = \tilde{\beta}_1^\dagger \mathbf{R}^b \tilde{\beta}_3 = 0. \quad (\text{B.7})$$

With (B.6), finally (B.5) reduces to

$$\bar{\Gamma}_{klil} = -\frac{1}{2} \tilde{\beta}_k^\dagger \mathbf{R}^f \tilde{\beta}_i \tilde{\beta}_i^\dagger \mathbf{R}^f \tilde{\beta}_l. \quad (\text{B.8})$$

This, together with (B.7) and (B.8), simplifies (B.3) into

$$B(\omega) = - \sum_{i=1}^3 \sum_{\substack{k=1 \\ k \neq i}}^3 \sum_{\substack{l=1 \\ l \neq i}}^3 \frac{\bar{\Gamma}_{klil}}{(\bar{\lambda}_i - \bar{\lambda}_k)(\bar{\lambda}_i - \bar{\lambda}_l)} \mathbf{a}^\dagger(\omega) \tilde{\beta}_k \tilde{\beta}_l^\dagger \mathbf{a}(\omega)$$

$$= \frac{1}{(\bar{\lambda}_2 - \bar{\lambda}_3)(\bar{\lambda}_2 - \bar{\lambda}_1)} \operatorname{Re} \left\{ \tilde{\beta}_3^\dagger \mathbf{R}^f \tilde{\beta}_2 \tilde{\beta}_2^\dagger \mathbf{R}^f \tilde{\beta}_1 a^\dagger(\omega) \tilde{\beta}_3 \tilde{\beta}_1^\dagger a(\omega) \right\}. \quad (\text{B.10})$$

Using (45) and (47), since

$$\tilde{\beta}_3^\dagger \mathbf{R}^f \tilde{\beta}_2 = j 2P M \sin 2(M-1) \tilde{\beta}_3^\dagger \mathbf{u}_1 \mathbf{u}_1^\dagger \tilde{\beta}_2$$

and

$$\tilde{\beta}_2^\dagger \mathbf{R}^f \tilde{\beta}_1 = -j 2P M \sin 2(M-1) \tilde{\beta}_2^\dagger \mathbf{u}_1 \mathbf{u}_1^\dagger \tilde{\beta}_1,$$

(B.10) can be expressed as

$$B(\omega) = \frac{4P^2 M^2 \sin^2 2(M-1)\omega_d}{(\bar{\lambda}_2 - \bar{\lambda}_1)(\bar{\lambda}_2 - \bar{\lambda}_3)} |\tilde{\beta}_2^\dagger \mathbf{u}_1|^2 \operatorname{Re} \left\{ \mathbf{u}_1^\dagger \tilde{\beta}_1 \tilde{\beta}_3^\dagger \mathbf{u}_1 a^\dagger(\omega) \tilde{\beta}_3 \tilde{\beta}_1^\dagger a(\omega) \right\}. \quad (\text{B.11})$$

Finally, with (B.2) and (B.11) we have the desired bias expression as

$$\begin{aligned} \bar{\eta}(\omega) &= \frac{\bar{\eta}_1 + \bar{\eta}_2}{N} + O\left(\frac{1}{N^2}\right) \\ &= \sum_{i=1}^3 \frac{\bar{\lambda}_i \sigma^2}{2N (\bar{\lambda}_i - \sigma^2)^2} \left\{ (M-3) |\tilde{\beta}_i^\dagger a(\omega)|^2 - \bar{Q}(\omega) \right\} + \frac{B(\omega)}{N} + O\left(\frac{1}{N^2}\right). \end{aligned} \quad (\text{B.12})$$

In a similar manner, the variance expression in (49) can be partitioned as

$$\begin{aligned} \operatorname{Var}(\hat{Q}(\omega)) &= \frac{2}{N} \sum_{i=1}^3 \sum_{j=1}^3 \left[\sum_{\substack{k=1 \\ k \neq i}}^3 \sum_{\substack{l=1 \\ l \neq j}}^3 q_{ijkl} + \sum_{\substack{k=1 \\ k \neq i}}^3 \sum_{l=4}^M q_{ijkl} \right. \\ &\quad \left. + \sum_{\substack{k=4 \\ k \neq i}}^M \sum_{\substack{l=1 \\ l \neq j}}^3 q_{ijkl} + \sum_{k=4}^M \sum_{l=4}^M q_{ijkl} \right] + O\left(\frac{1}{N^2}\right) \end{aligned} \quad (\text{B.13})$$

where

$$q_{ijkl} = \frac{\text{Re} \left[(\bar{\Gamma}_{klji} \mathbf{a}^\dagger(\omega) \bar{\beta}_j \bar{\beta}_l^\dagger \mathbf{a}(\omega) + \bar{\Gamma}_{kjli} \mathbf{a}^\dagger(\omega) \bar{\beta}_l \bar{\beta}_j^\dagger \mathbf{a}(\omega)) \mathbf{a}^\dagger(\omega) \bar{\beta}_k \bar{\beta}_i^\dagger \mathbf{a}(\omega) \right]}{(\bar{\lambda}_i - \bar{\lambda}_k)(\bar{\lambda}_j - \bar{\lambda}_l)}.$$

From the symmetry of the subscripts, the first term in (B.13) can be shown to be zero. Moreover, since $\bar{\beta}_i^\dagger \mathbf{R}^f (\mathbf{R}^b) \bar{\beta}_k = 0$ for $i \leq 3$ and $k \geq 4$, using the definition of $\bar{\Gamma}_{ijkl}$ in (50) the second and third terms in the above expression also turns out to be zero.

Now, we evaluate the fourth term in (B.13). For $i, j \leq 3$ and $k, l \leq 4$, we have

$$4\bar{\Gamma}_{klji} = \sigma^2 \delta_{kl} (\bar{\beta}_j^\dagger \mathbf{R}^f \bar{\beta}_i + \bar{\beta}_j^\dagger \mathbf{R}^b \bar{\beta}_i) = 2\bar{\lambda}_i \sigma^2 \delta_{kl} \delta_{ij} \quad (\text{B.14})$$

and

$$4\bar{\Gamma}_{kjli} = 2\bar{\lambda}_i \delta_{ij} (\bar{\beta}_k^\dagger \mathbf{R}^f \bar{\gamma}_l + \bar{\beta}_k^\dagger \mathbf{R}^b \bar{\gamma}_l) = 2\nu_{kl} \bar{\lambda}_i \sigma^2 \delta_{ij}, \quad (\text{B.15})$$

where we have made use of the identities $\bar{\gamma}_l = \mathbf{J} \bar{\beta}_l^* = \bar{\beta}_l$ for $l \leq 3$ that follow from (45) and (47) and

$$\bar{\beta}_k^\dagger \mathbf{R}^f (\text{or } \mathbf{R}^b) \bar{\gamma}_l = \bar{\beta}_k^\dagger \mathbf{R}^f (\text{or } \mathbf{R}^b) \left(\sum_{p=4}^M \nu_{pl} \bar{\beta}_p \right) = \sigma^2 \nu_{kl} \quad \text{for } l \geq 4.$$

Here ν_{kl} is an element of \mathbf{V}_1 . With (B.14) and (B.15) in (B.13), the variance can be simplified as [13]

$$\begin{aligned} \text{Var}(\hat{Q}(\omega)) &= \frac{2}{N} \sum_{i=1}^3 \sum_{j=1}^3 \sum_{k=4}^M \sum_{l=4}^M q_{ijkl} + O\left(\frac{1}{N^2}\right) \\ &= \frac{1}{N} \sum_{i=1}^3 \frac{\bar{\lambda}_i \sigma^2}{(\bar{\lambda}_i - \sigma^2)^2} \left[|\bar{\beta}_i^\dagger \mathbf{a}(\omega)|^2 \bar{Q}(\omega) + \sum_{k=4}^M \sum_{l=4}^M \text{Re}(\nu_{kl} \mathbf{a}^\dagger(\omega) \bar{\beta}_l \bar{\beta}_i^\dagger \mathbf{a}(\omega) \mathbf{a}^\dagger(\omega) \bar{\beta}_k \bar{\beta}_i^\dagger \mathbf{a}(\omega)) \right] + O\left(\frac{1}{N^2}\right) \\ &= \frac{2\bar{Q}(\omega)}{N} \sum_{i=1}^3 \frac{\bar{\lambda}_i \sigma^2}{(\bar{\lambda}_i - \sigma^2)^2} |\bar{\beta}_i^\dagger \mathbf{a}(\omega)|^2 + O\left(\frac{1}{N^2}\right). \end{aligned} \quad (\text{B.16})$$

Notice that this expression has structually the same form as that for the three uncorrelated-source scene in (7).

Appendix B

A New Spectrum Extension Method That Maximizes the Two-Step Prediction Error – Generalization of Maximum Entropy Method*

Abstract

Given $(n+1)$ consecutive autocorrelations of a stationary discrete-time stochastic process, one interesting question is how to extend this finite sequence so that the power spectral density associated with the resulting infinite sequence of correlations is nonnegative everywhere. It is well known that when the Hermitian Toeplitz matrix generated from the given correlations is positive-definite, the problem has an infinite number of solutions [1] and the particular solution that maximizes entropy results in a stable all-pole model of order n . Since maximization of entropy is equivalent to maximization of the minimum mean square error associated with one-step predictors [2], in this paper the problem of obtaining admissible extensions that maximize the minimum mean square error associated with k -step ($k \leq n$) predictors, that are compatible with the given correlations, is studied. It is shown here that the resulting spectrum corresponds to that of a stable ARMA $(n, k-1)$ process. The details of this true generalization of the maximum entropy extension are worked out here for a two-step predictor along with several other interesting conclusions.

I. Introduction

An interesting problem in the study of autocorrelation forms and their associated power spectral densities is that of estimating the spectrum from a finite extent of its correlation function. Known as the trigonometric moment problem in the discrete case, it has been the subject of extensive study for a long period [1 - 6]. In view of the considerable mathematical interest as well as the practical significance of the moment problem in interpolation theory, system identification, power gain approximation theory and spectrum estimation, it is appropriate to review the problem briefly in the present context. Towards this, let

* This work was supported by the Office of Naval Research under contract N-00014-89-J-1512.

$x(nT)$ represent a discrete-time, zero mean, wide sense stationary stochastic process with autocorrelation function,

$$r_k = E[x(nT) x^*((n+k)T)] = r_{-k}^*, \quad k = 0, 1, 2, \dots \infty. \quad (1)$$

As is well known, the power spectral density $S(\theta)$ of this stationary process is given by the discrete-time Fourier transform of its autocorrelation sequence [1], *i.e.*,

$$S(\theta) = \sum_{k=-\infty}^{+\infty} r_k e^{jk\theta}. \quad (2)$$

Moreover, $S(\theta) \geq 0$ and

$$r_k = \frac{1}{2\pi} \int_{-\pi}^{\pi} S(\theta) e^{-jk\theta} d\theta, \quad |k| \geq 0. \quad (3)$$

Clearly for processes with finite power, we have

$$\frac{1}{2\pi} \int_{-\pi}^{\pi} S(\theta) d\theta = r_0 = E[|x(t)|^2] < \infty, \quad (4)$$

i.e., $S(\theta)$ is integrable (belongs to L_1 over $-\pi \leq \theta \leq \pi$). The non-negativity property of the power spectral density can be characterized in terms of certain Toeplitz matrices generated from its correlations [2]. Let T_n denote the Hermitian Toeplitz matrix generated from $r_0, r_1, r_2, \dots, r_n$, and Δ_n its determinant. Thus,

$$T_n = \begin{bmatrix} r_0 & r_1 & r_2 & \cdots & r_n \\ r_1^* & r_0 & r_1 & \cdots & r_{n-1} \\ \vdots & \cdots & \cdots & \cdots & \vdots \\ r_n^* & r_{n-1}^* & \cdots & r_1^* & r_0 \end{bmatrix} \quad (5)$$

and⁽¹⁾

$$\Delta_n = \det T_n .$$

Then [2, 6]

$$S(\theta) \geq 0 \Leftrightarrow \Delta_n \geq 0 , \quad n = 0, 1, 2, \dots, \infty , \quad (6)$$

i.e., the nonnegativity property of the power spectral density function is equivalent to the nonnegative definiteness of all Hermitian Toeplitz matrices generated from its correlations.

Further, assume that the process also satisfies the Paley-Wiener criterion (causality criterion)⁽²⁾,

$$H = \frac{1}{2\pi} \int_{-\pi}^{\pi} \ln S(\theta) d\theta > -\infty , \quad (7)$$

i.e., the entropy H of this process is finite. With this additional constraint, it can be shown that [7 - 8] the nonnegative property of the power spectral density implies positive-definiteness for all T_n in (5), *i.e.*, $\Delta_n > 0$, $n = 0, 1, 2, \dots, \infty$.

The integrability condition in (4) together with the Paley-Wiener criterion permits the factorization of the power spectral density in terms of a unique function with certain interesting properties. In fact, in that case, there exists a unique function [7 - 9]

$$B(z) = \sum_{k=0}^{\infty} b_k z^k , \quad b_0 > 0 \quad (8)$$

that is analytic together with its inverse in $|z| < 1$, such that

(1) Here onwards a (or A), a and A stand for scalar, vector and matrix in that order. Similarly, A^* , A^T and A^\dagger represent the complex conjugate, transpose and complex conjugate transpose of A , respectively. The symbol $\det A = |A|$ is used to denote the determinant of the matrix A .

(2) From (4), the inequality $H < +\infty$ is automatically satisfied [8].

$$\sum_{k=0}^{\infty} |b_k|^2 < \infty \quad (9)$$

and⁽³⁾

$$S(\theta) = |B(e^{j\theta})|^2, \quad \text{a.e.} \quad (10)$$

This minimum phase factor $B(z)$ (free of zeros and poles in $|z| < 1$) is known as the Wiener factor of the given process and represents a causal, digital filter with square summable impulse response. Its physical meaning is not difficult to grasp. When driven by an appropriate stationary white noise source of unit spectral density, this filter regenerates the given stochastic process $x(nT)$, entirely from the past samples of the input white noise process (see Fig. 1).

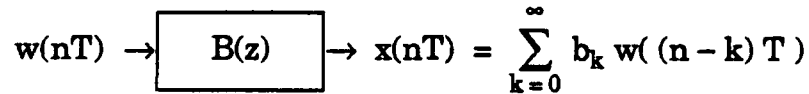


Fig. 1. Wiener Filter of a Stationary Process

We are in a position to state the spectrum extension problem: Given $(n+1)$ autocorrelations $r_0, r_1, r_2, \dots, r_n$, from a stationary stochastic process that satisfies (4) and (7), determine all solutions for the power spectral density $S(\theta)$ that are compatible with the given data; i.e., such a solution $S(\theta)$ should satisfy

$$S(\theta) \geq 0 \quad (11)$$

and

$$\frac{1}{2\pi} \int_{-\pi}^{\pi} S(\theta) e^{-jk\theta} d\theta = r_k, \quad k = 0, 1, 2, \dots, n, \quad (12)$$

(3) $B(e^{j\theta}) = \lim_{r \rightarrow 1-0} B(re^{j\theta})$. In addition to aesthetic reasons, the use of the variable z for the delay operator (in contrast to the usual z^{-1}), translates all stability arguments to be carried out in the compact region $|z| \leq 1$. Notice that $r_k, k = 0 \rightarrow \infty$ real guarantees $b_k, k = 0 \rightarrow \infty$ to be real; i.e., the Wiener factor for real processes are real.

in addition to satisfying (4) and (7).

It is well known that a necessary and sufficient condition for the existence of such a solution is the nonnegativity property of the Toeplitz matrix T_n generated by the given $(n + 1)$ correlations [2, 3]. Moreover, when T_n is positive definite (such is the case here), the above spectrum extension problem has an infinite number of solutions⁽⁴⁾ [3, 4]. Youla has parametrized this entire class of solutions for the spectral extension problem in a network theoretic setting in terms of bounded real⁽⁵⁾ (b.r) functions [10]. These solutions also follow from Schur's theory on b. r. functions [3]. Before examining them, to make further progress in the present context, it is necessary to gain some additional insight into the concepts such as maximization of entropy, prediction errors, and the Wiener factor.

Section II examines the maximum entropy extension and discusses its significance in terms of possessing a Wiener factor that maximizes the minimum mean square error associated with one-step predictors. Further, Youla's parametrization of the class of all extensions that are compatible with the given data, and their dependence on the maximum entropy solution [10] is briefly reviewed.

Given r_0, r_1, \dots, r_n , the Wiener factor that maximizes the minimum mean square error associated with a k -step predictor is shown to have an ARMA $(n, k-1)$ structure. The special case of the two-step predictor is treated in Section III and using an induction argument the general case is proved in Appendix A.

(4) When $\Delta_n = 0$, the above extension problem has a unique solution.

(5) $\rho(z)$ is said to be bounded real (b.r) if $|\rho(z)| \leq 1$ in $|z| < 1$ and is real for real z . By Cauchy's inequalities if $\rho(z) = \sum_{k=0}^{\infty} \rho_k z^k$, then $|\rho_k| < 1$ for all k . Further, if $|\rho_0| = 1$, then $\rho(z) = 1$.

Using Youla's parametric formulation, an explicit solution for the two-step predictor is worked out and presented in Section III.

II. Maximum Entropy Solution and the Class of All Extensions

A geometric interpretation of the class of admissible solutions is well known [1, 4, 5]. Clearly, under the hypothesis

$$\Delta_n = \begin{vmatrix} r_0 & r_1 & r_2 & \cdots & r_n \\ r_1^* & r_0 & r_1 & \cdots & r_{n-1} \\ \vdots & \cdots & \cdots & \cdots & \vdots \\ r_n^* & r_{n-1}^* & \cdots & \cdots & r_0 \end{vmatrix} > 0, \quad (13)$$

any admissible extension r_k , $k = n + 1 \rightarrow \infty$, should satisfy

$$\Delta_k > 0, \quad k = n + 1 \rightarrow \infty. \quad (14)$$

Consequently, at the first step $r_{n+1} = x$ must be chosen so that

$$\Delta_{n+1}(x) = \begin{vmatrix} r_0 & r_1 & \cdots & r_n & x \\ r_1^* & r_0 & r_1 & \cdots & r_n \\ \vdots & \cdots & \cdots & \cdots & \vdots \\ x^* & r_n^* & r_{n-1}^* & \cdots & r_0 \end{vmatrix} > 0. \quad (15)$$

Using well known matrix identities^(6, 7), $\Delta_{n+1}(\mathbf{x})$ can be expanded as

$$\Delta_{n-1} \Delta_{n+1}(\mathbf{x}) = \Delta_n^2 - \Delta_{n-1}^2 |\mathbf{x} - \xi_n|^2, \quad (16)$$

where

$$\xi_n = \gamma_f^\dagger \mathbf{T}_{n-1}^{-1} \gamma_b \quad (17)$$

$$\gamma_f \triangleq [r_1, r_2, \dots, r_n]^T,$$

and

$$\gamma_b \triangleq [r_n, r_{n-1}, \dots, r_1]^T.$$

In turn, (16) implies that, the set of values \mathbf{x} that satisfy (15) is the interior of a circle with radius

$$\lambda_n = \frac{\Delta_n}{\Delta_{n-1}} > 0 \quad (18)$$

and center ξ_n given by (17).

The general rule is now conceptually clear: Having selected $r_{n+1} = \mathbf{x}$ consistent with (15), r_{n+2} can be chosen from the interior of a circle with radius $\lambda_{n+1} = \Delta_{n+1}/\Delta_n$ and center ξ_{n+1} and so on. Notice that except for λ_n and ξ_n which are uniquely determined by the given data, all successive λ_k and ξ_k depend on the particular rule used to pick r_k from the interior of the respective circles $k = n+2 \rightarrow$

(6) Let \mathbf{A} be an $n \times n$ matrix and $A_{nw}, A_{ne}, A_{sw}, A_{se}$ denote the $(n-1) \times (n-1)$ minors formed from consecutive rows and consecutive columns in the northwest, northeast, southwest and southeast corners. Further let A_c denote the central $(n-2) \times (n-2)$ minor of \mathbf{A} . Then from a special case of an identity due to Jacobi [11],

$$A_c |\mathbf{A}| = A_{nw} A_{se} - A_{ne} A_{sw}$$

(7)

$$\begin{vmatrix} \mathbf{A} & \mathbf{B} \\ \mathbf{C} & \mathbf{D} \end{vmatrix} = |\mathbf{A}| |\mathbf{D} - \mathbf{C}\mathbf{A}^{-1}\mathbf{B}|$$

∞ . One particular choice, however, has several interesting properties. To observe this, first notice that⁽⁶⁾ for any k ,

$$\Delta_{k+1} = \frac{1}{\Delta_{k-1}} \left(|\Delta_k|^2 - |\Delta_{k+1}^{(1)}|^2 \right) \quad (19)$$

which gives the useful identity

$$\lambda_{k+1} = \frac{\Delta_{k+1}}{\Delta_k} = \frac{\Delta_k}{\Delta_{k-1}} \left(1 - \left| \frac{\Delta_{k+1}^{(1)}}{\Delta_k} \right|^2 \right) \leq \lambda_k. \quad (20)$$

Here, by definition $\Delta_{k+1}^{(1)}$ denotes the minor of Δ_{k+1} obtained by striking out its first column and last row. From (20), the sequence λ_k of positive numbers for $k = n \rightarrow \infty$ is always monotone nonincreasing and has a limit given by [7]

$$\lim_{k \rightarrow \infty} \lambda_k = \frac{\Delta_k}{\Delta_{k-1}} = b_0^2 > 0 \quad (21)$$

with b_0 as in (8) representing the constant term in the Wiener factor. Since $\lambda_k \leq \lambda_n$ for $k = n \rightarrow \infty$, this further implies that

$$b_0^2 \leq \lambda_n = \frac{\Delta_n}{\Delta_{n-1}} \quad (22)$$

with equality if and only if

$$\Delta_{k+1}^{(1)} = 0, \quad k = n \rightarrow \infty.$$

Or, equivalently, in that case

$$\lambda_k = \frac{\Delta_n}{\Delta_{n-1}}, \quad k = n \rightarrow \infty. \quad (23)$$

From (22), (23) and (16), b_0 assumes its maximum possible value

$$(b_0)_{\max} = \sqrt{\frac{\Delta_n}{\Delta_{n-1}}} \quad (24)$$

if and only if

$$x = r_{k+1} = \xi_k, \quad k = n \rightarrow \infty, \quad (25)$$

i.e., only when all extensions are at the centers of the respective admissible circles.

Since b_0^2 represents the minimum mean square error associated with a one-step predictor that makes use of the entire infinite past⁽⁸⁾ [2], the above completion rule suggests that the unique extension so obtained by identifying each r_k , $k = n + 1 \rightarrow \infty$ with the centers of the admissible circles also maximizes the minimum mean square error of a one-step predictor of the given process, *i.e.*, of all the one-step predictors that can be generated from each admissible completion, the one above has the maximum value for the minimum mean square prediction error and in that sense it is maximally robust. Interestingly, this is also the maximum entropy extension originally formulated by Burg [12, 13]. To see that the above extension also possesses maximum entropy among all possible extensions, it is enough to relate the entropy H of the process and the prediction error b_0^2 .

Towards this purpose let d_k , $|k| = 0, 1, 2, \dots, \infty$, represent the Fourier coefficients of $\ln S(\theta)$. Thus,⁽⁹⁾

$$d_k = \frac{1}{2\pi} \int_{-\pi}^{\pi} \ln S(\theta) e^{-jk\theta} d\theta \quad (26)$$

and hence [4]

$$\ln S(\theta) = \sum_{k=-\infty}^{\infty} d_k e^{jk\theta} \quad (27)$$

or

⁽⁸⁾ Using least mean square theory it follows that the best one step linear predictor

$\hat{x}(T) = \sum_{k=0}^{n-1} w_k x(-kT)$ that makes use of n past samples results in a mean square error

$\delta_n = \Delta_n / \Delta_{n-1}$. Clearly from (21), $\lim_{n \rightarrow \infty} \delta_n = b_0^2$.

⁽⁹⁾ The Paley-Wiener criterion (7) guarantees that $\ln S(\theta)$ is well defined almost everywhere.

$$S(\theta) = \exp(d_0) \exp\left(\sum_{k=1}^{\infty} d_k e^{jk\theta}\right) \exp\left(\sum_{k=1}^{\infty} d_k e^{jk\theta}\right)^* = L(e^{j\theta}) L^*(e^{j\theta}) \quad (28)$$

where

$$L(z) \triangleq \exp(d_0/2) \exp\left(\sum_{k=1}^{\infty} d_k z^k\right) \triangleq \exp(d_0/2) \sum_{k=0}^{\infty} \alpha_k z^k. \quad (29)$$

Clearly $\alpha_0 = 1$. On comparing (10) and (28), we can associate⁽¹⁰⁾ $L(z)$ with the Wiener factor $B(z)$, and in that case by equating (8) and (29), we obtain

$$b_k = \alpha_k \exp(d_0/2), \quad |k| \geq 0 \quad (30)$$

In particular, from (26) [2, 5, 6]

$$b_0^2 = \exp(d_0) = \exp\left(\frac{1}{2\pi} \int_{-\pi}^{\pi} \ln S(\theta) d\theta\right) = \exp(H) \quad (31)$$

This one-to-one relationship between entropy H and the one-step prediction error allows one to conclude that the above extension method that maximizes b_0^2 is also the maximum entropy extension. The maximum entropy solution plays a basic role in parametrizing all other admissible extensions. In a network theoretic setting involving positive-real (p.r.) functions, Youla has shown that, in the case of real correlations, every admissible solution $S(\theta)$ can be represented as [10].

$$S(\theta) = |B_p(e^{j\theta})|^2 \quad (32)$$

where, the Wiener factor $B_p(z)$ is given by

$$B_p(z) = \frac{\Gamma(z)}{D_n(z)}. \quad (33)$$

Here, $\Gamma(z)$ is a b.r. function, analytic together with its inverse in $|z| < 1$ (minimum

(10) Notice that $L(z)$ is also analytic together with its inverse in $|z| \leq 1$.

phase factor), that is associated with the spectral factorization

$$1 - |\rho(e^{j\theta})|^2 = |\Gamma(e^{j\theta})|^2$$

or, more compactly, with the factorization

$$1 - \rho(z) \rho_*(z) = \Gamma(z) \Gamma_*(z) \quad (34)$$

where, by definition

$$\rho_*(z) = \rho(1/z)$$

and $\rho(z)$ is an arbitrary bounded real function⁽⁵⁾. Further,

$$D_n(z) \triangleq P_n(z) - z\rho(z) \tilde{P}_n(z) \quad (35)$$

and $P_n(z)$ is the unique degree n polynomial generated by the Levinson algorithm from the given correlations $r_0, r_1, r_2, \dots, r_n$, through the recursion [14]:

$$\sqrt{1 - s_k^2} P_k(z) = P_{k-1}(z) - s_k z^k P_{k-1}(1/z), \quad k = 1, 2, \dots \quad (36)$$

Here $s_k, k = 1, 2, \dots$ are the reflection coefficients given by

$$s_k = (-1)^{k-1} \frac{\Delta_k^{(1)}}{\Delta_{k-1}} \quad (37)$$

with $\Delta_k^{(1)}$ as defined in (19)-(20). This recursion is carried out under the initialization

$$P_0(z) = \frac{1}{\sqrt{r_0}}$$

and

$$s_1 = \frac{r_1}{r_0}.$$

Interestingly, $P_n(z)$ can be compactly written as⁽¹¹⁾

(11) The Levinson recursion (36)-(37) follows from (38) through an easy determinant expansion⁽⁶⁾.

$$P_n(z) = \frac{1}{\sqrt{\Delta_n \Delta_{n-1}}} \begin{vmatrix} r_0 & r_1 & \cdots & \cdots & r_n \\ r_1^* & r_0 & \cdots & \cdots & r_{n-1} \\ \vdots & \cdots & \cdots & \cdots & \vdots \\ r_{n-1}^* & \cdots & \cdots & r_0 & r_1 \\ z^n & z^{n-1} & \cdots & z & 1 \end{vmatrix} \triangleq a_0 + a_1 z + a_2 z^2 + \cdots a_n z^n \quad (38)$$

and using Rouché's theorem [15] (or otherwise) on (36) and (35) repeatedly, through an induction argument it is easy to show that $P_n(z)$ and hence $D_n(z)$ are strict Hurwitz Polynomials.⁽¹²⁾ Moreover, by definition $\tilde{P}_n(z)$ represents the polynomial reciprocal to $P_n(z)$, i.e.,

$$\tilde{P}_n(z) = z^n P_n(1/z).$$

Thus, $\rho(z)$ b. r. implies that $B_\rho(z)$ is analytic together with its inverse in $|z| < 1$ with square summable Fourier coefficients. Clearly, $\rho(z)$ parametrizes $S(\theta)$ and moreover all these extensions satisfy the correlation matching property involving the first $(n+1)$ coefficients. In Youla's representation [10], all such spectral extensions can be realized as the real part (on the unit circle) of the input impedance of a cascade of $(n+1)$ lossless, equi-delay, transmission lines that has been terminated upon an arbitrary passive load $W(z)$. The transmission lines with characteristic impedances R_0, R_1, \dots, R_n , are generated from the given real correlations such that, the junction (mismatch) reflection coefficients $s_k = (R_k - R_{k-1}) / (R_k + R_{k-1})$, $k = 1, 2, \dots, n$, are given by (37) with $R_0 = r_0$. In this representation $\rho(z)$ represents the reflection coefficient of the load $W(z)$ at the far end normalized to the characteristic impedance R_n of the last line, i.e.,

(12) A Hurwitz Polynomial has all its zeros in $|z| \geq 1$. A strict Hurwitz polynomial has all its zeros in $|z| > 1$. Note that $r_k, k = 0 \rightarrow n$ real implies that the coefficients $a_k, k = 0 \rightarrow n$ in (38) are also real.

$$\rho(z) = \frac{W(z) - R_n}{W(z) + R_n} . \quad (39)$$

To obtain the maximum entropy solution explicitly, we proceed to evaluate the entropy H_p associated with the general solution(32) and maximize it with respect to the free parameter $\rho(z)$. Since

$$H_p = \frac{1}{2\pi} \int_{-\pi}^{\pi} \ln S(\theta) d\theta = \ln b_0^2 ,$$

from (8) and (32)

$$b_0^2 = B_p^2(0) = \frac{\Gamma^2(0)}{D_n^2(0)} = \frac{\Gamma^2(0)}{P_n^2(0)} = \Gamma^2(0) \frac{\Delta_n}{\Delta_{n-1}} \quad (40)$$

and using (24), (31)

$$H_p = \ln \frac{\Delta_n}{\Delta_{n-1}} - \ln [1/\Gamma^2(0)] = H_{ME} - \ln [1/\Gamma^2(0)] . \quad (41)$$

Clearly the extension that maximizes entropy is the one where $\Gamma(0) = 1$. Since $\Gamma(z)$ is also b.r., notice that $\Gamma^2(0) < 1$ unless $\Gamma(z) \equiv 1$, and consequently $\Gamma(0) = 1$ implies⁽⁵⁾ $\rho(z) \equiv 0$. In Youla's representation, this is equivalent to terminating the last line on its characteristic impedance R_n (see (39)). Thus from (32) – (35) the maximum entropy spectral extension has the form

$$S(\theta) = \frac{1}{|P_n(e^{j\theta})|^2} \quad (42)$$

and the associated Wiener factor

$$B_{ME}(z) = \frac{1}{P_n(z)} = \frac{1}{a_0 + a_1 z + a_2 z^2 + \dots + a_n z^n} \quad (43)$$

represents a stable AutoRegressive form of order n (i.e., AR(n)). Alternatively, van den Bos has shown that [16] the standard linear prediction method⁽⁸⁾ also leads to

the same set of Yule-Walker equations as the maximum entropy method and hence (43) also represents the best linear prediction filter. From (32), (33) and (35) the polynomial $P_n(z)$ that characterizes the maximum entropy solution plays a key role in all other extensions, and in particular, the one that maximizes the two-step prediction error.

III. The Wiener Factor that Maximizes the Two-Step Prediction Error

Given the correlations $r_0, r_1, r_2, \dots, r_n$, of all the admissible completions given by (32) and (33), the problem here is to find the one that maximizes the k -step minimum mean square prediction error. In what follows, we first deal with the two-step predictor case. It is shown here that maximization of the two-step prediction error results in an ARMA $(n, 1)$ process. Through a constructive procedure, the existence of the ARMA $(n, 1)$ Wiener factor is demonstrated for this case. The general case is dealt with in Appendix A, where it is shown that maximization of the k -step minimum mean square error results in an ARMA $(n, k-1)$ process.

Using (29) and (30), the two-step prediction error P_2 is given by [2],

$$P_2 = |b_0|^2 + |b_1|^2 = [1 + |\alpha_1|^2] \exp \left[\frac{1}{2\pi} \int_{-\pi}^{\pi} \ln S(\theta) d\theta \right]. \quad (44)$$

Naturally, maximization of P_2 is with respect to the unknown autocorrelations $r_{n+1}, r_{n+2}, r_{n+3}, \dots$ and using the relation $\alpha_1 = d_1 = \frac{1}{2\pi} \int_{-\pi}^{\pi} \ln S(\theta) e^{-j\theta} d\theta$, this leads to

$$\frac{\partial P_2}{\partial r_k} = \frac{1}{2\pi} \int_{-\pi}^{\pi} \left[\frac{(1 + |\alpha_1|^2) + \alpha_1 e^{j\theta} + \alpha_1^* e^{-j\theta}}{S(\theta)} \right] e^{jk\theta} d\theta$$

$$= \frac{1}{2\pi} \int_{-\pi}^{\pi} \frac{|1 + \alpha_1 e^{j\theta}|^2}{S(\theta)} e^{jk\theta} d\theta = 0, \quad |k| > n. \quad (45)$$

Clearly, (45) implies that the Fourier series expansion for the real periodic nonnegative function $|1 + \alpha_1 e^{j\theta}|^2/S(\theta)$ truncates after the n th term and hence it must have the form

$$\frac{|1 + \alpha_1 e^{j\theta}|^2}{S(\theta)} = \sum_{k=-n}^n c_k e^{jk\theta} = \left| \sum_{k=0}^n g_k e^{jk\theta} \right|^2 \quad (46)$$

or

$$S(\theta) = \frac{|1 + \alpha_1 e^{j\theta}|^2}{\left| \sum_{k=0}^n g_k e^{jk\theta} \right|^2} = |B_2(e^{j\theta})|^2 \quad (47)$$

where

$$B_2(z) = \frac{A(z)}{G(z)}, \quad (48)$$

$$A(z) = (1 + \alpha_1 z) \quad \text{or} \quad \left(1 + \frac{1}{\alpha_1^*} z\right) \quad (49)$$

and

$$G(z) = \sum_{k=0}^n g_k z^k. \quad (50)$$

Thus, at least formally $B_2(z) \sim \text{ARMA}(n, 1)$, i.e., the Wiener factor that maximizes the two step prediction error, if it exists, is of the type $\text{ARMA}(n, 1)$. To complete the argument, we must demonstrate the existence of such a factor that is analytic together with its inverse in $|z| < 1$.

Toward this purpose, notice that in the case of real correlations, this specific extension, if admissible, should follow from (32) for a certain choice of the

bounded-real function $\rho(z)$ and in that case, on comparing (48) and (33), because of degree restrictions, the simplest $\rho(z)$ must have the form⁽¹³⁾

$$\rho(z) = \frac{1}{a + bz} . \quad (51)$$

For (51) to be bounded real, it is necessary that there exist no poles in $|z| < 1$, i.e.,

$$\left| \frac{a}{b} \right| > 1 , \quad (52)$$

and

$$\left| \frac{1}{a + b e^{j\theta}} \right| \leq 1 \Leftrightarrow (a \pm b)^2 \geq 1 , \quad (53)$$

(in addition to a and b being real).

Conversely, when (52) and (53) is true, from maximum modulus theorem [17], analyticity in $|z| < 1$, together with (53) implies boundedness for $\rho(z)$ in $|z| \leq 1$. In the present situation, the existence of such a b. r. function as in (51) can be verified by solving for a, b from (34) - (35) and examining whether they satisfy the necessary and sufficient conditions (52) and (53). In that case, through a direct calculation, the degree n requirement for $G(z)$ yields,

$$b = \frac{a_0}{a_n} , \quad (54)$$

$$\Gamma(z) = \frac{\alpha + \beta z}{a + bz} \quad (55)$$

where α, β satisfies

$$\alpha^2 + \beta^2 = a^2 + b^2 - 1 \quad (56)$$

$$\alpha\beta = ab \quad (57)$$

(13) It is shown in Appendix B that $\rho(z) = \frac{1 + dz}{a + bz + cz^2}$ etc, are not acceptable. (Note that $B_p(z)$ rational implies that $\rho(z)$ must be rational.)

and

$$D_n(z) = \frac{\left(\sum_{k=0}^n g_k z^k \right)}{a + bz} \quad (58)$$

with

$$g_k = a_{k-1} b + a_k a - a_{n-k+1}, \quad k = 0, 1, 2, \dots, n. \quad (59)$$

Here a_k , $k = 0, 1, 2, \dots, n$, are the coefficients of $P_n(z)$ (see (38)). Moreover, the Wiener factor $B_2(z)$ yields the power series expansion (in $|z| < 1$),

$$B_2(z) = \frac{\alpha + \beta z}{\sum_{k=0}^n g_k z^k} = \frac{\alpha}{g_0} + \left(\frac{\beta}{g_0} - \frac{\alpha g_1}{g_0^2} \right) z + \dots \triangleq b_0 + b_1 z + b_2 z^2 + \dots \quad (60)$$

and hence from (29)-(30)

$$\alpha_1 = \frac{b_1}{b_0} = \left(\frac{\beta}{\alpha} - \frac{g_1}{g_0} \right). \quad (61)$$

On the other hand, from (48)-(49) and (60)

$$\alpha_1 = \frac{\beta}{\alpha} \quad \text{or} \quad \frac{\alpha}{\beta} \quad (62)$$

(since $b_k, \alpha_k, k = 0 \rightarrow \infty$ are real in the case of real correlations). It is easy to show that the first choice $\alpha_1 = \beta/\alpha$ does not always lead to a bounded real solution for $\rho(z)$. In fact, by letting $\alpha_1 = \beta/\alpha$ and equating this to (61), we obtain $g_1 / g_0 = 0$, which in turn implies $g_1 = 0$ since $g_0 = a_0 a$ is a finite number, i.e.,

$$g_1 = a_0 b + a_1 a - a_n = 0$$

or

$$a = \frac{a_n - a_0 b}{a_1} = \frac{a_n^2 - a_0^2}{a_1 a_n}$$

which gives

$$\frac{a}{b} = \frac{a_n^2 - a_0^2}{a_0 a_1}.$$

From (52), for $\rho(z)$ to be b.r., $|a/b| > 1$. However as the strict Hurwitz polynomial $P_2(z) = (z+2)(2z+3) = 2z^2 + 7z + 6$ shows

$$\left| \frac{a}{b} \right| = \frac{6^2 - 2^2}{6 \times 7} = \frac{32}{42} < 1$$

and hence, from (52), $\alpha_1 = \beta/\alpha$ is not an appropriate choice.⁽¹⁴⁾ Turning back to (62), this leads to the only other possibility

$$\alpha_1 = \frac{\alpha}{\beta}. \quad (63)$$

Equating (61) and (63), we obtain

$$\frac{\beta^2 - \alpha^2}{\alpha\beta} = \frac{g_1}{g_0}. \quad (64)$$

Using (56), (57) and (59) and after some algebra, (64) reduces to the cubic equation with real coefficients

$$x^3 + px + q = 0, \quad (65)$$

where

$$x = \frac{a}{b}, \quad (66)$$

$$p = -2 \left(1 + \frac{1}{b^2} + \frac{a_1^2}{2a_0^2} \right) < 0 \quad (67)$$

and

⁽¹⁴⁾ At times, the above choice can lead to admissible solutions. For example, in the case of the strict Hurwitz polynomial $P_2(z) = 5 - 2z + z^2$, the parameters a, b so obtained generate a b. r. $\rho(z)$ leading to an admissible Wiener factor.

$$q = -\frac{2a_1}{a_0} \left(1 - \frac{1}{b^2}\right). \quad (68)$$

Clearly, the Wiener factor $B_2(z)$ in (60) that maximizes the two-step prediction error represents an admissible solution, if the cubic equation (65) has at least one real solution with magnitude greater than unity and further that solution together with (54) satisfies (53). To examine this, notice that if the discriminant

$$D = \left(\frac{q}{2}\right)^2 + \left(\frac{p}{3}\right)^3 \quad (69)$$

is negative, then (65) has three real roots and if $D > 0$ it has one real root and two complex roots that form a conjugate pair [18]. However, as shown in Appendix B, the above discriminant is always negative and the corresponding three real roots can be obtained explicitly by making use of Cardano's formula. In that case, let

$$R = \operatorname{sgn}(q) \left(-\frac{p}{3}\right)^{1/2} = -\operatorname{sgn}\left(\frac{a_1}{a_0}\right) \sqrt{\frac{2}{3} \left(1 + \frac{1}{b^2} + \frac{a_1^2}{2a_0^2}\right)}. \quad (70)$$

Then, the three roots are given by [18]

$$\begin{aligned} x_1 &= -2R \cos(\varphi/3) \\ x_2 &= -2R \cos(\varphi/3 + 2\pi/3) \end{aligned} \quad (71)$$

and

$$x_3 = -2R \cos(\varphi/3 + 4\pi/3)$$

where

$$\cos \varphi = \frac{q}{2R^3} = \frac{\left|\frac{a_1}{a_0}\right| \left(1 - \frac{1}{b^2}\right)}{\left[\frac{2}{3} \left(1 + \frac{1}{b^2} + \frac{a_1^2}{2a_0^2}\right)\right]^{3/2}}. \quad (72)$$

It is easy to show that two of these roots always have magnitude greater than

unity. This follows from a well-known sufficiency condition due to Cohn⁽¹⁵⁾, which in the case of (65) reduces to $|p| > |q| + 1$, for two of its roots to have magnitude greater than unity. To verify this condition, notice that

$$\begin{aligned} |p| - |q| - 1 &= 2 \left(1 + \frac{1}{b^2} + \frac{a_1^2}{2a_0^2} \right) - 2 \left| \frac{a_1}{a_0} \right| \left(1 - \frac{1}{b^2} \right) - 1 \\ &= \left(1 - \left| \frac{a_1}{a_0} \right| \right)^2 + \frac{2}{b^2} \left(1 + \left| \frac{a_1}{a_0} \right| \right) > 0 \end{aligned} \quad (73)$$

and hence (65) has two roots with magnitude greater than unity and one with magnitude less than unity. Moreover, without exception⁽¹⁶⁾, $\cos \varphi \geq 0$, which implies $|\varphi| < \pi/2$ or

$$\cos \left(\frac{\varphi}{3} \right) > \cos \left(\frac{\pi}{6} \right) = \frac{\sqrt{3}}{2}, \quad (74)$$

and

$$\frac{1}{2} < -\cos \left(\frac{\varphi}{3} + \frac{2\pi}{3} \right) < \frac{\sqrt{3}}{2}, \quad -\cos \left(\frac{\varphi}{3} + \frac{4\pi}{3} \right) < \frac{1}{2}. \quad (75)$$

Thus, x_2 and x_3 have the same sign that is opposite to the sign of x_1 . Clearly, the sign of x_2 and x_3 is the same as that of q . The structure of these roots is summarized in Fig. 2. Further, since $|R| > \sqrt{2/3}$, using (74) and (75) we also have $2|R| > |x_1| > \sqrt{3}|R|$, $\sqrt{3}|R| > |x_2| > |R|$ and $|x_3| < |R|$ which gives

$$|x_1| > |x_2| > |x_3|. \quad (76)$$

Thus, using the Cohn criterion, x_1 and x_2 have magnitudes greater than unity, i.e., $\rho(z)$ obtained using any one of these roots is always analytic in $|z| \leq 1$.

(15) For a polynomial $f(z) = a_0 + a_1 z + \dots + a_p z^p + \dots + a_n z^n$, $a_p \neq 0$, if $|a_p| > |a_0| + |a_1| + \dots + |a_{p-1}| + |a_{p+1}| + \dots + |a_n|$, then $f(z)$ has exactly p zeros inside the unit circle [15].

(16) $|b| = |a_0 / a_n| > 1$, since a_0 / a_n represents the product of the n -roots of the strict Hurwitz polynomial $P_n(z)$.

For bounded reality, it remains to show that a, b so obtained from these roots also satisfy

$$(a \pm b)^2 \geq 1.$$

In what follows, we will first demonstrate this condition for the largest root⁽¹⁷⁾ x_1 .

In that case, using (66), (70) and (74), x_1 gives rise to

$$|a^{(1)}| \triangleq |x_1| |b| \geq \sqrt{3} |R| |b| = \sqrt{2 \left(1 + b^2 + \frac{a_1^2}{2a_n^2} \right)} > 2$$

Again, without loss of generality, we can assume $a^{(1)}$ and b are of the same sign – say positive (i.e., $x_1 > 0, b > 1$) – and hence,

$$(a^{(1)} + b)^2 > 9 > 1. \quad (77)$$

To verify the second part, let

$$(a^{(1)} - b)^2 \geq \left(\sqrt{2 \left(1 + b^2 + \frac{a_1^2}{2a_n^2} \right)} - b \right)^2 = \Delta^2 \quad (78)$$

To find its minimum, notice that by straightforward algebra $\frac{\partial \Delta}{\partial b} = 0$ yields

$$\tilde{b}_0^2 = 1 + \frac{a_1^2}{2a_n^2}.$$

But, the second derivative

$$\frac{\partial^2 \Delta}{\partial b^2} = \frac{\sqrt{2} \left(1 + \frac{a_1^2}{2a_n^2} \right)}{\left(\sqrt{1 + b^2 + \frac{a_1^2}{2a_n^2}} \right)^3}$$

⁽¹⁷⁾ Since $|x_3| < 1$, there can atmost be two solutions, one corresponding to x_1 and the other corresponding to x_2 . The solution due to x_2 is discussed later.

is always positive and hence, in particular, at $\tilde{b}_0^2 = 1 + \frac{a_1^2}{2a_n^2}$, the quantity Δ in (78)

achieves its minimum value given by

$$\Delta_{\min} = \sqrt{2(2\tilde{b}_0^2) - \tilde{b}_0} = \tilde{b}_0$$

or

$$(a^{(1)} - \tilde{b}_0)^2 \geq \Delta_{\min}^2 = \tilde{b}_0^2 > 1.$$

This completes the proof. The uniqueness for this choice of $\rho(z)$ is proved in Appendix C.

To investigate the solution due to x_2 , notice that under the above assumptions ($x_1 > 0, b > 1$), x_2 and hence $a^{(2)} = x_2 b$ are negative and as a result $|a^{(2)} - b| > 1$ is automatically satisfied. For bounded reality of the $\rho(z)$ so obtained from $a^{(2)}$ and b , it remains to show that $|a^{(2)} + b| \geq 1$. Towards proving this, let $y = a + b = b(a/b + 1) = b(x + 1)$ or $x = (y/b) - 1$ and substituting this in (65) yields the polynomial

$$V(y) = y^3 - 3by^2 + (3+p)b^2y + (-1-p+q)b^3.$$

Let y_1, y_2 and y_3 denote the three real roots of this cubic equation. We will show that all these roots have magnitudes greater than unity. In fact, from (77) and the assumptions, we have $y_1 = a^{(1)} + b > 1$ and further using (73), $V(0) = (-1-p+q)b^3 > 0$. Since one of its roots y_1 is greater than unity and the ordinate-intercept is positive, to establish the above claim, it is enough to show that $V(1) > 0$ and $V(-1) > 0$. In that case, due to its cubic nature, $V(y)$ must have the shape shown in Fig. 3(a) which corresponds to a strict Hurwitz polynomial. An easy manipulation shows that

$$V(1) = (b-1) \left(\frac{a_1}{a_n} - 1 - b \right)^2 > 0$$

and

$$V(-1) = (b+1) \left(\frac{a_1}{a_n} + 1 - b \right)^2 > 0,$$

which, in particular, establishes that $|y_2| = |a^{(2)} + b| > 1$. Thus, $\rho_2(z) = 1 / (a^{(2)} + bz)$ also leads to a b. r. function and consequently to a solution to the original problem.

To complete the proof, it remains to exhaust the remaining choices for b and x_1 , viz ; ($b > 1$, $x_1 < 0$; $b < -1$, $x_1 > 0$; $b < -1$, $x_1 < 0$). Of these, for example, when $b > 1$ and $x_1 < 0$, we have $a^{(1)} < 0$ and $a^{(2)} > 0$ and $a^{(3)} > 0$ and hence $|a^{(2)} + b| > 1$ is automatic. In that case, we need $|a^{(2)} - b| > 1$ and letting $z = a - b = b(x - 1)$ or $x = (z/b) + 1$, leads to the new cubic equation

$$W(z) = z^3 + 3bz^2 + (3+p)b^2z + (1+p+q)b^3.$$

Once again since $z_1 = a^{(1)} - b < -1$ and $W(0) < 0$, to prove $|z_2| > 1$, it is enough to show that $W(1) < 0$ and $W(-1) < 0$. In fact,

$$W(1) = -(b+1) \left(\frac{a_1}{a_n} - 1 + b \right)^2 < 0$$

and

$$W(-1) = -(b-1) \left(\frac{a_1}{a_n} - 1 + b \right)^2 < 0$$

and this situation corresponds to that in Fig. 3(b). Thus, $|z_2| = |a^{(2)} - b| > 1$, etc.⁽¹⁸⁾

The remaining case can be dealt with in a similar manner. Notice that, to determine the bounded reality for $\rho_2(z)$, we have made use of the previously established fact that $|a^{(1)} \pm b| > 1$.

The general case involving complex correlations can be dealt with in a similar manner. In that case, to exhibit an admissible solution, it is enough to

(18) Interestingly, the above arguments also establish that $|a^{(3)} \pm b| > 1$. However, this is irrelevant, since $|x_3| < 1$.

demonstrate the existence of a bounded function ($\rho(z)$ is bounded if $|\rho(z)| \leq 1$ in $|z| < 1$).

Figures 4-6 together with Tables 1-3 show details of maximum entropy extension and the two-step predictors discussed above in three different situations. In Fig. 4, the original spectrum corresponds to an autoregressive model of order 6 and the number of known Fourier coefficients is taken to be 7. As pointed out in the Conclusions (Section IV), the maximum entropy extension results in the same autoregressive form as the original one and the maximally robust two-step predictors generate stable ARMA(6, 1) forms with spectra as shown in Fig. 4 (c). The dotted curve represents the spectrum corresponding to x_1 and the solid curve that due to x_2 . The corresponding filter coefficients are tabulated in Table 1. In Figs. 5 and 6, the original spectra correspond to those of ARMA(8, 1) and ARMA(6, 3) processes respectively. In both cases the number of known Fourier coefficients is taken to be $p + 1$, where p corresponds to the respective denominator degree. The associated maximum entropy extension as well as the best two-step predictor extensions are shown in Fig. 5 (b)-(c), Fig. 6 (b)-(c), and the corresponding filter coefficients are tabulated in Table 2 and Table 3, respectively. Notice that in all these cases, the dotted curve appears to be 'closer' to the maximum entropy extension, while the solid one tends to 'follow' the original one. This is not surprising, since, from the discussions in Section IV, the entropy corresponding to the dotted curve is greater than that of the solid one and consequently the dotted curve is 'closer' to the maximum entropy extension. However, since these extensions only possess a single zero, they cannot truly approximate spectra containing a larger number of zeros.

To summarize, through a constructive procedure we have demonstrated the existence of two Wiener factors that maximize the minimum mean square error associated with two-step predictors that are compatible with the given

correlations r_0, r_1, \dots, r_n . They turn out to be stable⁽¹⁹⁾ ARMA $(n, 1)$ filters given by

$$B_2(z) = \frac{\alpha + \beta z}{\sum_{k=0}^n g_k z^k}$$

where

$$\alpha = \frac{1}{2} [\sqrt{(a+b)^2 - 1} + \sqrt{(a-b)^2 - 1}],$$

$$\beta = \frac{1}{2} [\sqrt{(a+b)^2 - 1} - \sqrt{(a-b)^2 - 1}],$$

with

$$a = -2bR \cos\left(\frac{\phi}{3}\right) \text{ or } -2bR \cos\left(\frac{\phi}{3} + \frac{2\pi}{3}\right), \quad (79)$$

and

$$b = \frac{a_0}{a_n},$$

and $g_k, k = 0 \rightarrow n$, as given in (59). Further, R and ϕ are as in (70) and (72), respectively. As remarked earlier, the two choices for the parameter a in (79) give rise to two bounded-real functions and two admissible Wiener factors.

IV. Conclusions

In this paper, through a constructive procedure, we have demonstrated the existence of two admissible power spectra with the property that the associated Wiener factors maximize the minimum mean square error among the class of all two-step predictors, that are compatible with the given $(n+1)$ correlations of a stationary stochastic process. Maximization of the two-step prediction error is

(19) Note that $D_n(z)$ is strict Hurwitz so long as $\rho(z)$ is b. r.

shown to result in two unique and stable ARMA (n, 1) filters with details as given in section III. This is a true generalization of Burg's maximum entropy extension which results in a stable AR (n) filter.

As remarked before, from a geometric viewpoint, the maximum entropy extension is also maximally robust because the new estimates so obtained are always at the centers of the admissible circles (see (25)). As a result, in that case the radius b_0 of 'the final circle' has the maximum possible value $\sqrt{\Delta_n / \Delta_{n-1}}$. Naturally, any other extension cannot have all its new estimates at the centers of admissible circles and from (20) - (22), it now follows that the radius of 'the final circle' for any other admissible extension will be strictly less than that corresponding to the maximum entropy extension. Thus, the radius of 'the final circle' may be taken as a measure of the robustness for the extension under consideration. In the case of ARMA(n, 1) extension, from (21) and (60), the 'final radius' is given by

$$b_0 = \frac{\alpha}{g_0} = \left(\frac{\sqrt{(a+b)^2 - 1} + \sqrt{(a-b)^2 - 1}}{2a} \right) \sqrt{\frac{\Delta_n}{\Delta_{n-1}}} \geq \frac{1}{\sqrt{2}} \sqrt{\frac{\Delta_n}{\Delta_{n-1}}} , \quad (80)$$

where $|a| > |b| + 1$ and $|b| > 1$. Since the radii of admissible circles form a monotone nonincreasing sequence, this implies that all ARMA (n, 1) extensions have a 'final radius', which is at least 70% of the maximum possible value. Since the specific ARMA (n, 1) extension discussed in Section III maximizes the two-step prediction error $(|b_0|^2 + |b_1|^2)$, the final radius in that case should possess a tighter lower bound.

Given a finite number of covariances, so far we have demonstrated two admissible Wiener factors that maximize the two-step prediction error by exhibiting two b. r. functions from the real roots of a cubic equation. The special structure of the numerator part of the Wiener factor in (48) together with its

general form in (33) gave rise to the above cubic constraint that must be satisfied by all admissible b. r. functions. The particular solutions presented in Section III involve two of its roots – the largest ones in magnitude – and since there are two admissible candidates, this raises the natural question : Does the particular solution given above using the largest root have any unique property?

Interestingly, in such a situation, the solution corresponding to the largest root possesses greater entropy (i.e., larger 'final radius') and in that sense it is most robust among the two solutions. This follows easily by noticing that the entropy $H(a)$ of an ARMA (n, 1) admissible extension is given by $H(a) = \ln b_0^2$, with b_0 as in (80) where a and b as a pair satisfy $|a| > |b| + 1$, $|b| = |a_0 / a_n| > 1$. In that case, it is easy to show that $\partial H / \partial a > 0$ and further $a = \infty$ is its only stationary point. Hence, $H(a)$ is a monotone increasing function of a. Referring back to (76), since $a^{(1)} = x_1 b$ is larger than $a^{(2)} = x_2 b$ in magnitude, we have $H(a^{(1)}) > H(a^{(2)})$ proving our assertion. In this sense, the ARMA(n, 1) extension characterized by the largest root in Section III is unique : it maximizes the two-step prediction error and possesses maximum entropy between the two admissible solutions.

The uniqueness of the above ARMA (n, 1) should not be confused with other admissible ARMA (n, 1) extensions. In fact, from (51), with b as given by (54) and, for example, letting $|a| > |b| + 1$ results in a bounded real function $p(z)$ that generates an admissible ARMA (n, 1) extension. Thus, there is an infinite number of admissible ARMA (n, 1) extensions that match the first (n+1) correlations, and the particular one described above is distinguished by the fact that it is most robust (maximizes the minimum mean square two-step prediction error and has maximum entropy) among all such ARMA (n, 1) admissible extensions.

The existence of a single AR (n) type of extension as well as the abundance of admissible ARMA (n, 1) extensions that match the given (n+1) correlations

follow from a general result on Padé approximations [19]. More generally, given $n = (p + q + 1)$ correlations, an ARMA (p, q) admissible extension, if it exists, is unique, *i.e.*, there can be only one admissible extension of the ARMA (p, q) type that matches the first $(p + q + 1)$ correlations. Of course, if $n < (p + q + 1)$, then the admissible extensions need not be unique.

Finally, given a set of $(n+1)$ correlations, the question of maximizing the entropy among all admissible ARMA $(n, 1)$ type extensions is also interesting by itself. From (31) and (80), this is equivalent to maximizing the above b_0 with respect to the variable a . As pointed out before, $\partial b_0 / \partial a = 0$ results in the solution $a = \infty$ and this does not lead to a realizable b.r. solution $\rho(z)$. Thus, given $(n+1)$ autocorrelations, an ARMA $(n, 1)$ type admissible extension that maximizes entropy does not exist.

Further, the natural generalization to k -step predictors ($k > 2$) that maximize the corresponding minimum mean square error is shown to result in a structured ARMA $(n, k-1)$ filter in Appendix A. In general, to identify an ARMA (p, q) system, $(p+q+1)$ correlations are needed. But if fewer correlations are to be used to identify the same system, then this approach leads to a feasible solution. In that case, beginning with $(p+1)$ correlations, maximization of $(q+1)$ -step prediction error leads to an ARMA (p, q) solution. The parametrization of such filters is, of course, much more complicated.

Appendix. A

Maximization of the k -step Prediction Error

Given a finite set of $(n+1)$ autocorrelations $r_0, r_1, r_2, \dots, r_n$, the problem here is to find the extension that maximizes the minimum mean square error associated with the k -step predictor. Using (29) and (30), the k -step minimum

mean square prediction error is given by

$$P_k = \sum_{i=0}^{k-1} |b_i|^2 = e^{d_0} (1 + |\alpha_1|^2 + |\alpha_2|^2 + \dots + |\alpha_{k-1}|^2) \quad (\text{A.1})$$

with d_0 as defined in (26). Maximization of P_k with respect to the free parameters r_{n+1}, r_{n+2}, \dots leads to

$$\frac{\partial P_k}{\partial r_m} = 0, \quad |m| > n$$

and using (A.1), this is equivalent to

$$\frac{\partial d_0}{\partial r_m} \left(\sum_{i=0}^{k-1} |\alpha_i|^2 \right) + \frac{\partial}{\partial r_m} \left(\sum_{i=0}^{k-1} |\alpha_i|^2 \right) = 0, \quad |m| > n. \quad (\text{A.2})$$

We will show that the left hand side of the above expression reduces to

$$\frac{1}{2\pi} \int_{-\pi}^{\pi} \frac{1}{S(\theta)} \left| \sum_{i=0}^{k-1} \alpha_i e^{ji\theta} \right|^2 e^{jm\theta} d\theta \quad (\text{A.3})$$

and this in turn implies that the periodic function given by (A.3) is identically equal to zero for all $|m| > n$. As a result, the nonnegative periodic function

$\frac{1}{S(\theta)} \left| \sum_{i=0}^{k-1} \alpha_i e^{ji\theta} \right|^2$ must truncate after n -terms and hence

$$\frac{1}{S(\theta)} \left| \sum_{i=0}^{k-1} \alpha_i e^{ji\theta} \right|^2 = \sum_{i=-n}^n f_i e^{ji\theta} = \left| \sum_{i=0}^n g_i e^{ji\theta} \right|^2$$

or

$$S(\theta) = \frac{\left| \sum_{i=0}^{k-1} \alpha_i e^{ji\theta} \right|^2}{\left| \sum_{i=0}^n g_i e^{ji\theta} \right|^2} = |B_k(e^{j\theta})|^2 \quad (\text{A.4})$$

where

$$B_k(z) = \frac{\sum_{i=0}^{k-1} \alpha_i z^i}{\sum_{i=0}^n g_i z^i} \quad \sim \text{ARMA}(n, k-1). \quad (\text{A.5})$$

Thus, to complete the proof, it is enough to establish the equality between the left-hand side of (A.2) and (A.3). Towards this, from (26), we obtain

$$\frac{\partial d_0}{\partial r_m} = \frac{1}{2\pi} \int_{-\pi}^{\pi} \frac{1}{S(\theta)} e^{jm\theta} d\theta \quad (\text{A.6})$$

and by direct expansion

$$\left| \sum_{i=0}^{k-1} \alpha_i e^{ji\theta} \right|^2 = \sum_{i=0}^{k-1} |\alpha_i|^2 + \sum_{p=0}^{k-1} \sum_{q=0}^{p-1} 2 \operatorname{Re} \left(\alpha_p e^{jp\theta} \alpha_q^* e^{-jq\theta} \right). \quad (\text{A.7})$$

Substituting (A.6) in (A.2) and (A.7) in (A.3), the desired equality condition between (A.2) and (A.3) reduces to

$$\sum_{p=0}^{k-1} \frac{\partial}{\partial r_m} |\alpha_p|^2 = \frac{1}{2\pi} \int_{-\pi}^{\pi} \sum_{p=0}^{k-1} \sum_{q=0}^{p-1} 2 \operatorname{Re} \left(\alpha_p e^{jp\theta} \alpha_q^* e^{-jq\theta} \right) e^{jm\theta} d\theta, \quad |m| > n. \quad (\text{A.8})$$

However,

$$\sum_{p=0}^{k-1} \frac{\partial}{\partial r_m} |\alpha_p|^2 = \sum_{p=0}^{k-1} \frac{\partial}{\partial r_m} \left| \alpha_p e^{jp\theta} \right|^2 = \sum_{p=0}^{k-1} 2 \operatorname{Re} \left\{ \alpha_p e^{jp\theta} \cdot \frac{\partial}{\partial r_m} \left(\alpha_p e^{-jp\theta} \right) \right\}$$

and hence with the above expression in (A.8), a term by term comparison simplifies (A.8) into

$$\frac{\partial}{\partial r_m} \left(\alpha_p^* e^{-jp\theta} \right) = \frac{1}{2\pi} \int_{-\pi}^{\pi} \frac{1}{S(\theta)} \left(\sum_{q=0}^{p-1} \alpha_q^* e^{-jq\theta} \right) e^{jm\theta} d\theta, \quad (\text{A.9})$$

where $|m| > n$ and $0 < p \leq k-1$.

We will establish (A.9) through an induction argument on p . To avoid cumbersome notations, we will assume (A.9) is true up to $p = k-1$ and will extend that result to $p = k$. Clearly (A.9) is well known for $k = 1$ and is proved for $k = 2$ in Section III. To make further progress for $k > 2$, notice that with α_k and d_k as defined in (29), straightforward algebra gives the useful identity [1, 10]

$$\alpha_k = \frac{1}{k} \left(d_1 \alpha_{k-1} + 2 d_2 \alpha_{k-2} + \dots + (k-1) d_{k-1} \alpha_1 + k d_k \alpha_0 \right), \quad k > 1. \quad (\text{A.10})$$

and hence

$$\begin{aligned} \frac{\partial \alpha_k^*}{\partial r_m} &= \frac{1}{k} \left[\sum_{i=1}^k \frac{\partial d_i^*}{\partial r_m} \alpha_{k-i}^* + \sum_{i=1}^{k-1} d_i^* \frac{\partial \alpha_{k-i}^*}{\partial r_m} \right] \\ &= \frac{1}{k} \left[\sum_{i=1}^k \alpha_{k-i}^* \cdot \frac{1}{2\pi} \int_{-\pi}^{\pi} \frac{i e^{ji\theta}}{S(\theta)} e^{jm\theta} d\theta + \sum_{i=1}^{k-1} i d_i^* \frac{\partial \alpha_{k-i}^*}{\partial r_m} \right] \end{aligned}$$

where we have made use of (26) and the identity $\alpha_0 = 1$. By assumption, since (A.9) is true for $p = k-1$, substituting that into the above expression, we obtain

$$\frac{\partial \alpha_k^* e^{-jk\theta}}{\partial r_m} = \frac{1}{2\pi} \int_{-\pi}^{\pi} \frac{A(\theta)}{S(\theta)} e^{jm\theta} d\theta \quad (\text{A.11})$$

where

$$A(\theta) = 1 + \frac{1}{k} \left[\sum_{i=1}^{k-1} i \left(\alpha_{k-i}^* e^{-j(k-i)\theta} + d_i^* e^{ji\theta} \sum_{q=0}^{k-i-1} \alpha_q^* e^{-jq\theta} \right) \right]. \quad (\text{A.12})$$

Expanding the terms in (A.12) and rearranging them with the help of (A.10), it simplifies into $\sum_{i=0}^k \alpha_i e^{-ji\theta}$. This establishes the identity (A.9) for $p = k$, and completes the proof.

Thus, given $r_0, r_1, r_2, \dots, r_n$, the Wiener factor that maximizes the k -step minimum mean square prediction error, has the form

$$B_k(z) = \frac{\sum_{m=0}^{k-1} \alpha_m z^m}{\sum_{m=0}^n g_m z^m} \sim \text{ARMA}(n, k-1).$$

Notice that the coefficients in the numerator factor here are precisely those given by (29) and moreover, from (33), this extension should also follow for a specific choice of rational $\rho(z)$ with numerator degree $(k-2)$ and denominator degree $(k-1)$. The denominator degree requirement for $B_k(z)$ together with the above restrictions on its numerator factor completely specifies the b. r. function $\rho(z)$ and hence the Wiener factor. For the existence of such a Wiener factor, the set of equations so obtained must yield a b. r. solution. Whether this is always possible for $k \geq 3$, is still an open question.

Appendix B

In this appendix, we will show that the discriminant D in (69) is always negative. To prove this, with (67) - (68) in (69) and letting $a_1^2 / a_0^2 = y$, the discriminant D simplifies into

$$D = \left(\frac{q}{2}\right)^2 + \left(\frac{p}{3}\right)^3$$

$$= \frac{5}{9} \left(1 + \frac{1}{b^4}\right) y - \frac{26}{9b^2} y - \frac{1}{27} \left[y^3 + 6 \left(1 + \frac{1}{b^2}\right) y^2 + 8 \left(1 + \frac{1}{b^2}\right)^3 \right], \quad y > 0. \quad (\text{B.1})$$

Since $|b| > 1$, we have $\frac{1}{|b|} < 1$, which gives $\frac{y}{b^4} < \frac{y}{b^2}$ and with this in the above expression, it simplifies into

$$D \leq \frac{5}{9} y - \frac{7}{3b^2} y - \frac{1}{27} \left[y^3 + 6 \left(1 + \frac{1}{b^2}\right) y^2 + 8 \left(1 + \frac{1}{b^2}\right)^3 \right] = -\frac{7}{3b^2} y - \frac{A(y)}{27}, \quad (\text{B.2})$$

where, by definition

$$A(y) = y^3 + 6 \left(1 + \frac{1}{b^2}\right) y^2 - 15y + 8 \left(1 + \frac{1}{b^2}\right)^3. \quad (\text{B.3})$$

Clearly, to establish $D < 0$, it is enough to show that $A(y) > 0$ for all $y > 0$ and $|b| > 1$.

Let $\beta = 2 \left(1 + \frac{1}{b^2}\right)$, then $|b| > 1$ implies $2 < \beta < 4$ and (B.3) simplifies into

$$A(y) = y^3 + 3\beta y^2 - 15y + \beta^3. \quad (\text{B.4})$$

The desired result follows if $A_{\min} > 0$ for $y > 0$ and $2 < \beta < 4$. To find its minimum, note that

$$\frac{\partial A(y)}{\partial y} = 3y^2 + 6\beta y - 15 = 0$$

yields the positive solution

$$y_0 = -\beta + \sqrt{\beta^2 + 5}$$

and the minimum value for (B.4) is given by

$$A(y_0) = 3\beta^3 - 2(\beta^2 + 5)\sqrt{\beta^2 + 5} + 15\beta = A_0(\beta). \quad (\text{B.5})$$

As Fig. 7 shows $A(y_0) > 0$ for $2 < \beta < 4$ and this completes the proof.

Appendix C

Uniqueness of $\rho(z)$

For uniqueness of $\rho(z)$ in (51), it remains to show that other feasible forms such as

$$\rho(z) = \frac{1 + d_1 z + d_2 z^2 + \dots + d_{m-1} z^{m-1}}{a + bz + c_1 z^2 + c_2 z^3 + \dots + c_{m-1} z^m}, \quad m > 1 \quad (C.1)$$

cannot give rise to bounded real functions of degree one in (48), unless $c_i = d_i = 0$, $i = 1, 2, \dots, m-1$. To prove this, consider first

$$\rho(z) = \frac{1 + dz}{a + bz + cz^2}. \quad (C.2)$$

From (33), since $B_2(z) = \Gamma(z)/D_n(z)$, the degree one requirement in the numerator of the Wiener factor $B_2(z)$ in (48), translates into the same requirement for the numerator of $\Gamma(z)$. Thus with (C.2) in (34), we obtain

$$(a + bz + cz^2)(a + bz + cz^2)_* - (1 + dz)(1 + dz)_* = (\alpha + \beta z)(\alpha + \beta z)_*$$

which is the same as

$$ac(z^2 + z^{-2}) + (ab + bc - d)(z + z^{-1}) + a^2 + b^2 + c^2 - d^2 - 1 = \alpha\beta(z + z^{-1}) + \alpha^2 + \beta^2.$$

Comparing the equal powers of z on both sides, we must have either $a = 0$ or $c = 0$.

If $a = 0$, then

$$\rho(z) = \frac{1 + dz}{z(b + cz)}$$

and it is not a b. r. function because of the pole at the origin. On the other hand, if $c = 0$, then

$$\rho(z) = \frac{1 + dz}{a + bz}$$

and substituting this in (35), we obtain

$$D_n(z) = \frac{-da_0z^{n+2} + (ba_n - a_0 + da_1)z^{n+1} + \dots}{a + bz}.$$

Since $D_n(z)$ is of degree n , necessarily $da_0 = 0 \Rightarrow d = 0$, since $a_0 \neq 0$ and this leads to

$$\rho(z) = \frac{1}{a + bz}. \quad (C.3)$$

Arguing in a similar manner, starting with any $m > 2$, (C.1) can be shown to reduce to (C.3). This proves our claim.

Acknowledgement

The first author wishes to acknowledge his deep gratitude to Professor Dante C. Youla of Polytechnic, for the many discussions on this and other related topics.

V. References

- [1] N. I. Ahiezer and M. Krein, *Some Questions in the Theory of Moments*, American Math. Society, Math. Monograph, vol. 2, 1962.
- [2] U. Grenander and G. Szegő, *Toeplitz Forms and Their Applications*. New York: Chelsea, 1984.
- [3] J. Schur, "Über Potenzreihen, die im innern des Einheitskreises beschränkt sind," *Journal für Reine und Angewandte Mathematik*, vol. 147, pp. 205-232, 1917; also vol. 148, pp. 122-145, 1918.
- [4] Ya. L. Geronimus, *Polynomials Orthogonal on a Circle*, American Math. Society Translation, no. 104, 1954.

- [5] J. A. Shohat and J. D. Tamarkin, *The Problem of Moments*, American Math., Society, Math. Surveys, no. 1, 1970.
- [6] G. Szegő, *Orthogonal Polynomials*, American Mathematical Society Colloquium Publications, vol. 23, 1985.
- [7] D. C. Youla and N. N. Kazanjian, "Bauer-type factorization of positive matrices and the theory of matrix polynomials orthogonal on the unit circle," *IEEE Trans. Circuits Sys.*, vol. CAS-25, pp. 57-69, February 1978.
- [8] N. Wiener and P. Masani, "*The prediction theory of multivariate processes, Part I: 'The regularity condition,'*" *Acta. Math.* vol. 98, 1957.
- [9] I. Gikhman and V. Skorokhod, *Introduction to the Theory of Random Processes*, Philadelphia: W. B. Saunders Company, 1965.
- [10] D. C. Youla, "The FEE: A new tunable high-resolution spectral estimator," Part I, Technical note no. 3, Department of Electrical Engineering, Polytechnic Institute of New York, Brooklyn, New York, 1980.
- [11] D. P. Robbins and H. Ru, "Determinants and Alternating Sign Matrices," *Advances in Mathematics*, vol. 62, pp. 169-184, 1986.
- [12] J. P. Burg, "Maximum entropy analysis," presented at the 37th Annual Meeting, Soc. Explor. Geophysics, Oklahoma City, Oklahoma, 1967.
- [13] J. P. Burg, *Maximum Entropy Spectral Analysis*, Ph.D. dissertation, Stanford University, Stanford, CA, May, 1975.
- [14] G. Szegő, *Collected Papers*, vol. 3, R. Askey Ed. Boston: Birkhäuser, 1982.
- [15] M. Marden, *The Geometry of the Zeros of a Polynomial in a Complex Variable*, American Math. Society, Math. Surveys, no. 3, 1949.
- [16] A. van den Bos, "Alternative interpolation of maximum entropy spectral analysis," *IEEE Trans. Inform. Theory*, vol. IT-17, pp. 493-494, July 1971.
- [17] P. Dienes, *The Taylor Series*, New York: Dover Publications, 1957.

- [18] J. V. Uspensky, *Theory of Equations*, 1st. ed., New York: McGraw-Hill Book Co., 1948.
- [19] G. A. Baker, Jr., *Essentials of Pade Approximants*, New York: Academic Press, 1975.

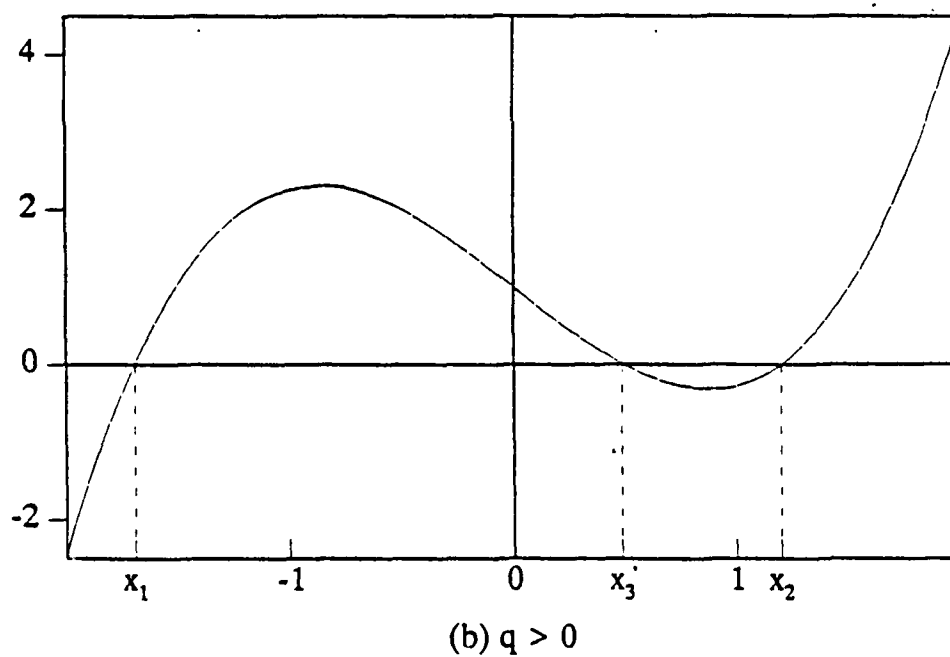
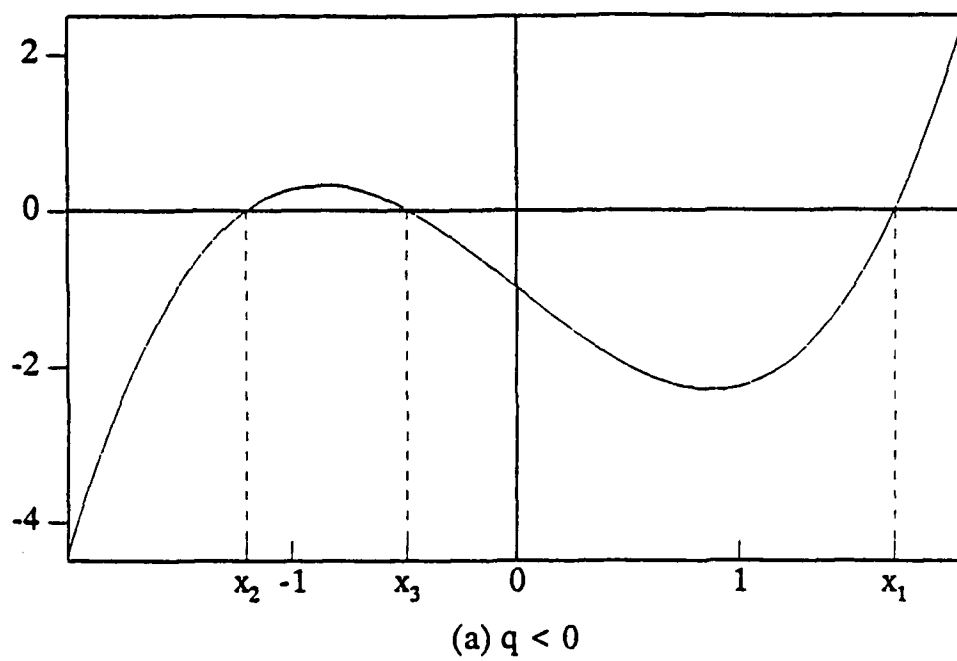


Fig. 2 Structure of the cubic function $x^3 + px + q$, $p < 0$ (see (65)-(68)).

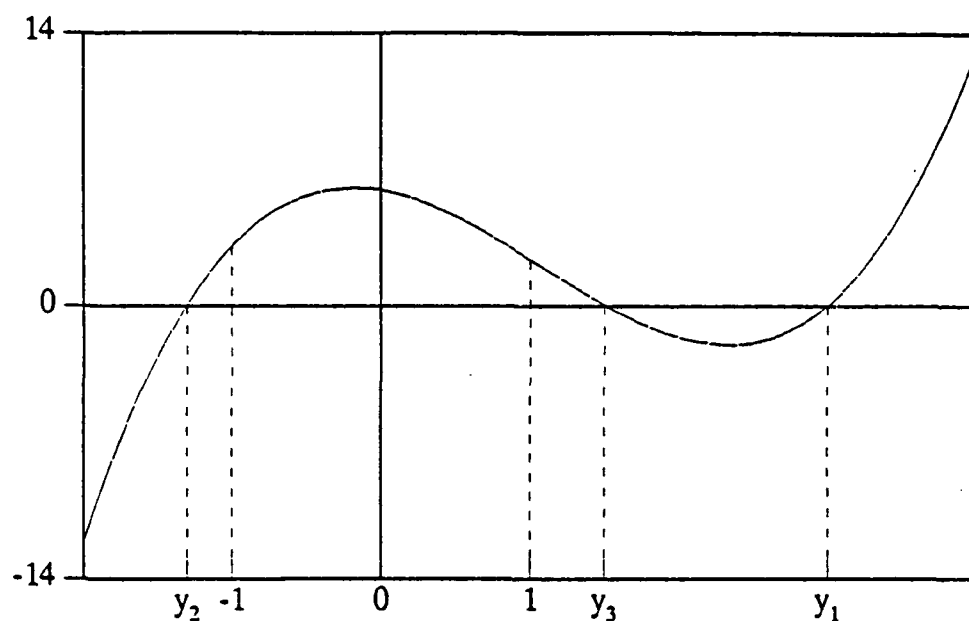


Fig. 3(a) $V(y) = y^3 - 3by^2 + (3+p)b^2y + (-1-p+q)b^3$; $b > 1, x_1 > 0$.
 $V(0)$, $V(1)$ and $V(-1)$ are all positive.

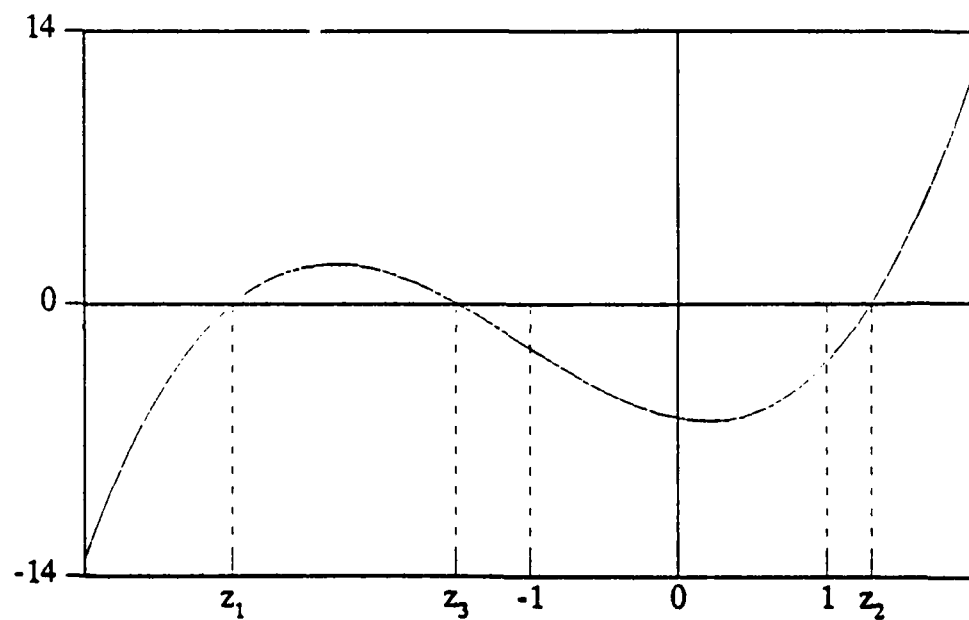


Fig. 3(b) $W(z) = z^3 + 3bz^2 + (3+p)b^2z + (1+p+q)b^3$; $b > 1, x_1 < 0$.
 $W(0)$, $W(1)$ and $W(-1)$ are all negative.

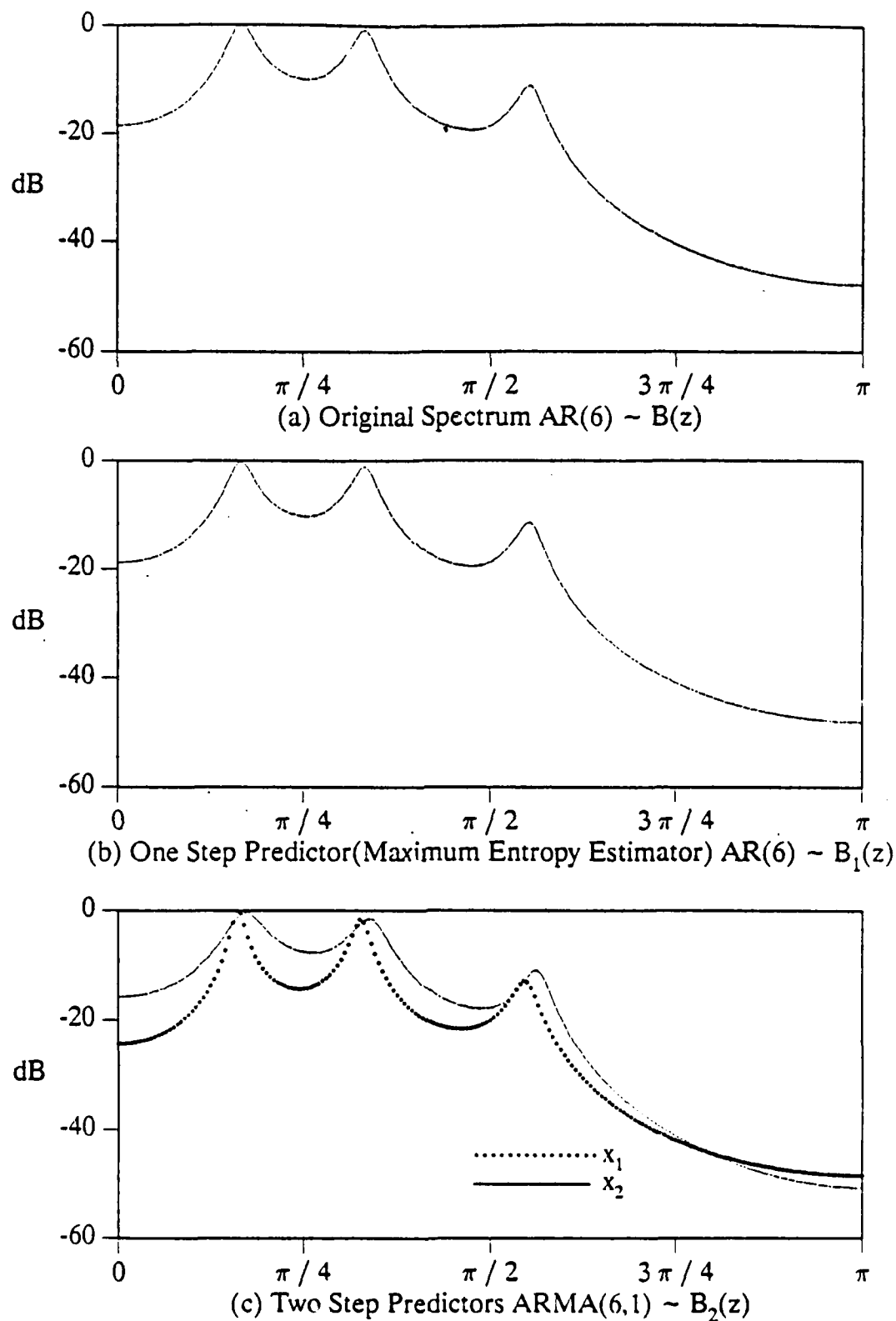


Fig. 4 One and two step predictors that maximize the minimum mean square error. Original spectrum corresponds to an Autoregressive model of order 6 given by

$$B(z) = \frac{1}{1.340 - 3.044z + 4.599z^2 - 4.825z^3 + 4.171z^4 - 2.504z^5 + z^6}$$

The number of Fourier coefficients known is taken to be 7.

Table 1

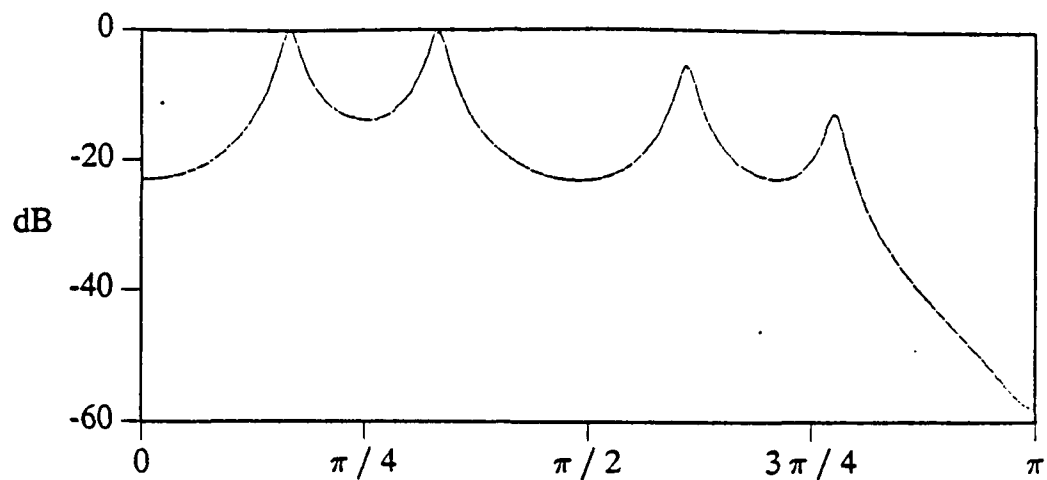
**One-Step and Two-Step Predictors
that Maximize the Minimum Mean Square Error**

$$B(z) = \frac{Q(z)}{P(z)} ; B_1(z) = \frac{Q_1(z)}{P_1(z)} ; B_2(z) = \frac{Q_2(z)}{P_2(z)} .$$

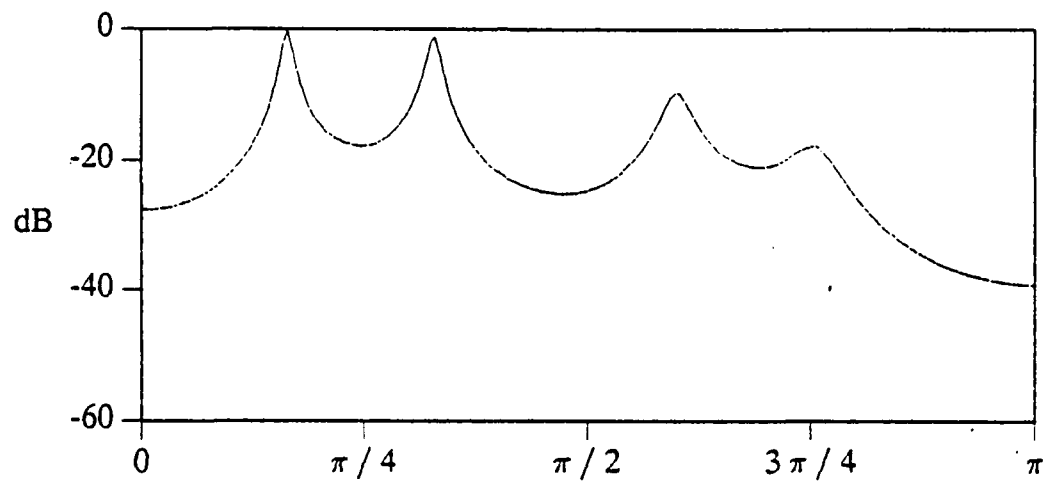
$B(z)$, $B_1(z)$ and $B_2(z)$ represent the original, the one-step and two-step Wiener factors, respectively.

n = No. of Fourier coefficients used for (b) and (c).

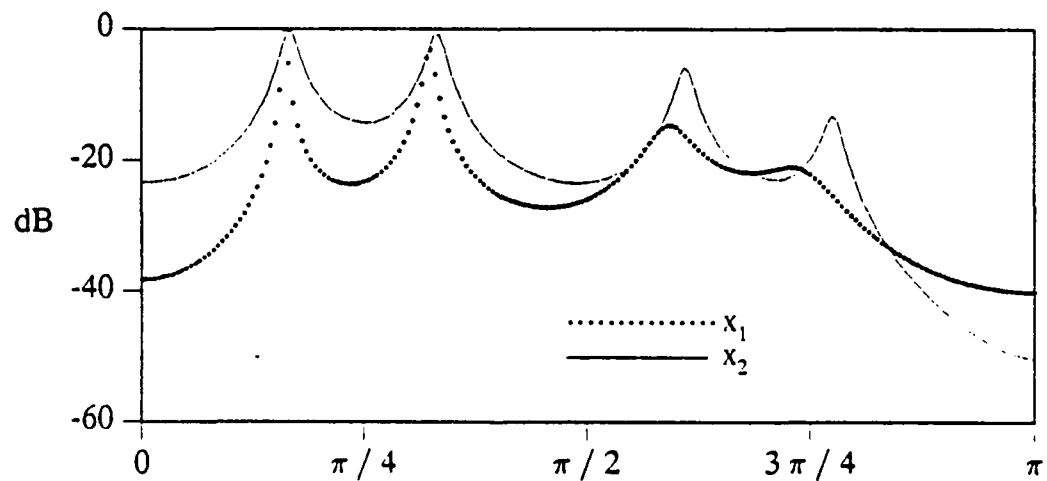
Fig.No.		n	Model	Wiener Factor Coefficients
Fig.4	a (original)	7	AR(6)	$Q(z) = 1$ $P(z) = 1.340 - 3.044z + 4.599z^2 - 4.825z^3 + 4.171z^4 - 2.504z^5 + z^6$
	b		AR(6)	$Q_1(z) = 1$ $P_1(z) = 1.340 - 3.044z + 4.599z^2 - 4.825z^3 + 4.171z^4 - 2.504z^5 + z^6$
	c (dotted)		ARMA(6,1)	$Q_2(z) = -0.895 + 0.322z$ $P_2(z) = 1.243 - 3.009z + 4.632z^2 - 4.948z^3 + 4.250z^4 - 2.553z^5 + z^6$
	c (solid)		ARMA(6,1)	$Q_2(z) = 1.044 + 0.416z$ $P_2(z) = 1.464 - 3.089z + 4.557z^2 - 4.680z^3 + 4.070z^4 - 2.442z^5 + z^6$



(a) Original Spectrum ARMA(8,1) ~ B(z)



(b) One Step Predictor(Maximum Entropy Estimator) AR(8) ~ B₁(z)



(c) Two Step Predictors ARMA(8,1) ~ B₂(z)

Fig. 5 One and two step predictors that maximize the minimum mean square error. Original spectrum corresponds to an ARMA(8,1) given by

$$B(z) = \frac{1.1 + z}{1.267 - 0.635z + 0.366z^2 - 0.664z^3 + 1.425z^4 - 0.626z^5 + 0.770z^6 - 0.531z^7 + z^8}$$

The number of Fourier coefficients known is taken to be 9.

Table 2

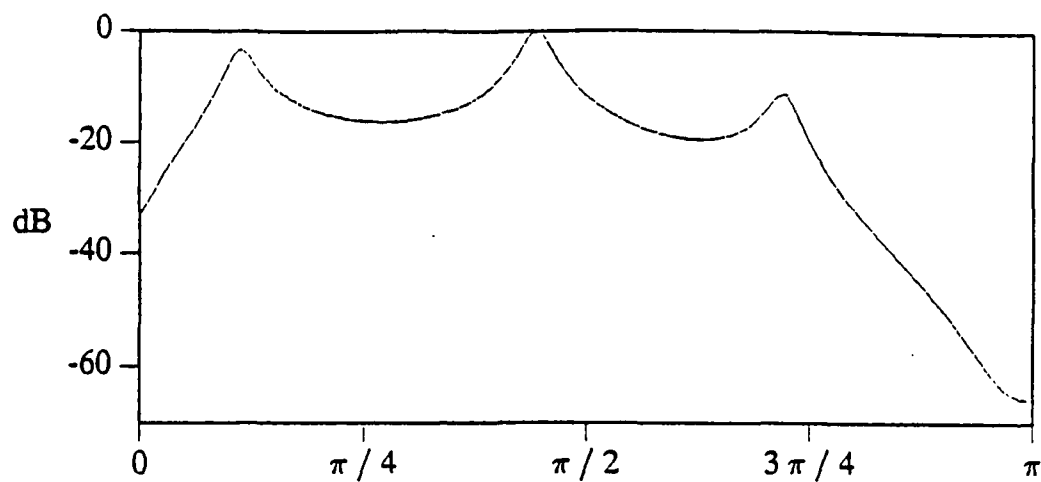
**One-Step and Two-Step Predictors
that Maximize the Minimum Mean Square Error**

$$B(z) = \frac{Q(z)}{P(z)} ; B_1(z) = \frac{Q_1(z)}{P_1(z)} ; B_2(z) = \frac{Q_2(z)}{P_2(z)} .$$

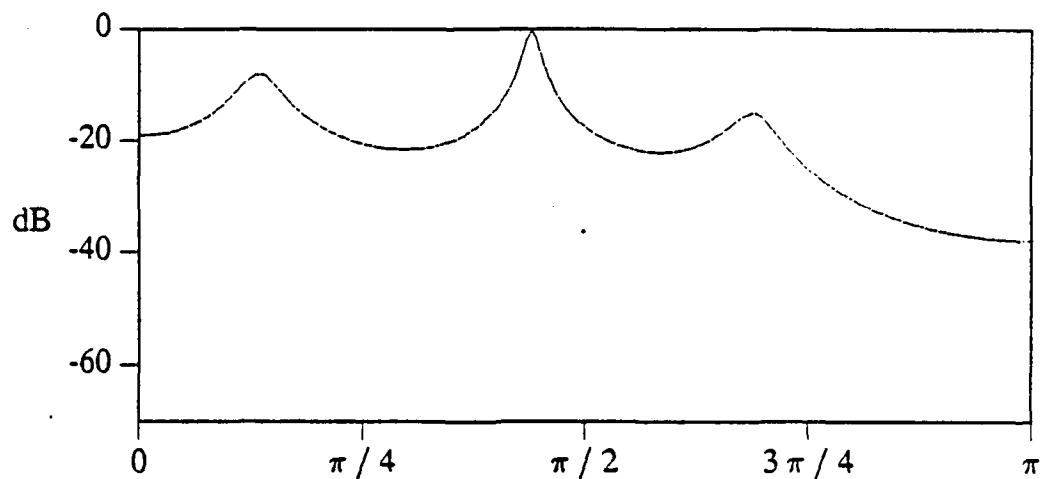
$B(z)$, $B_1(z)$ and $B_2(z)$ represent the original, the one-step and two-step Wiener factors, respectively.

n = No. of Fourier coefficients used for (b) and (c).

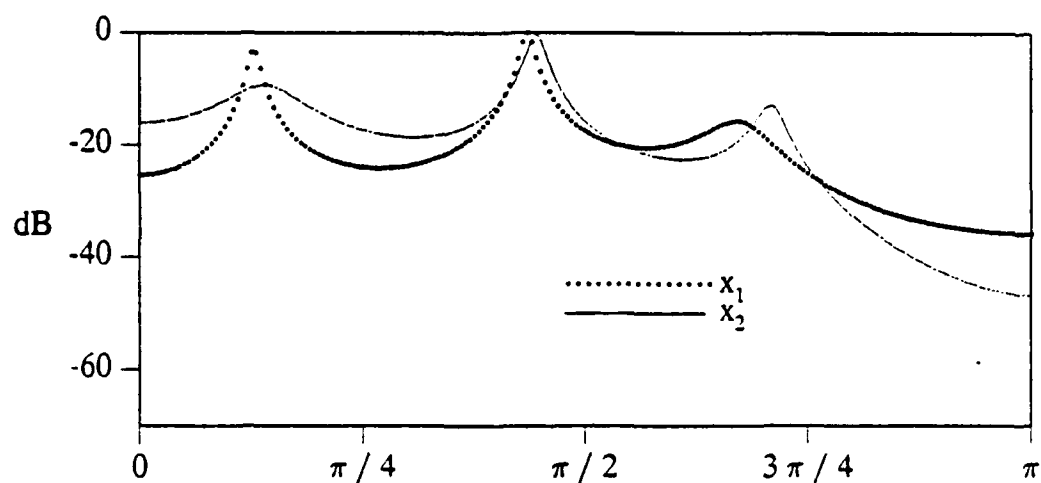
Fig.No.	n	Model	Wiener Factor Coefficients
Fig.5	a (original)	ARMA(8,1)	$Q(z) = 1.1 + z$ $P(z) = 1.267 - 0.635z + 0.866z^2 - 0.664z^3 + 1.425z^4 - 0.626z^5 + 0.770z^6 - 0.531z^7 + z^8$
	b	AR(8)	$Q_1(z) = 1$ $P_1(z) = 1.411 - 1.115z + 1.367z^2 - 1.132z^3 + 1.830z^4 - 1.007z^5 + 0.976z^6 - 0.663z^7 + z^8$
	c (dotted)	ARMA(8,1)	$Q_2(z) = -1.004 + 0.610z$ $P_2(z) = 1.563 - 1.623z + 1.898z^2 - 1.627z^3 + 2.258z^4 - 1.410z^5 + 1.194z^6 - 0.663z^7 + z^8$
	c (solid)	ARMA(8,1)	$Q_2(z) = 0.766 + 0.594z$ $P_2(z) = 1.272 - 0.651z + 0.883z^2 - 0.680z^3 + 1.439z^4 - 0.639z^5 + 0.777z^6 - 0.533z^7 + z^8$



(a) Original Spectrum ARMA(6,3) ~ B(z)



(b) One Step Predictor (Maximum Entropy Estimator) AR(6) ~ B₁(z)



(c) Two Step Predictors ARMA(6,1) ~ B₂(z)

Fig. 6 One and two step predictors that maximize the minimum mean square error. Original spectrum corresponds to an ARMA(6,3) given by

$$B(z) = \frac{-1.317 - 1.089z + 1.181z^2 + z^3}{1.340 - 1.201z + 0.961z^2 - 1.208z^3 + 0.871z^4 - 0.988z^5 + z^6}$$

The number of Fourier coefficients known is taken to be 7.

Table 3

**One-Step and Two-Step Predictors
that Maximize the Minimum Mean Square Error**

$$B(z) = \frac{Q(z)}{P(z)} ; B_1(z) = \frac{Q_1(z)}{P_1(z)} ; B_2(z) = \frac{Q_2(z)}{P_2(z)} .$$

$B(z)$, $B_1(z)$ and $B_2(z)$ represent the original, the one-step
and two-step Wiener factors, respectively.

n = No. of Fourier coefficients used for (b) and (c).

Fig.No.		n	Model	Wiener Factor Coefficients
Fig.6	a (original)	7	ARMA(6,3)	$Q(z) = -1.317 - 1.089z + 1.181z^2 + z^3$ $P(z) = 1.340 - 1.201z + 0.961z^2 - 1.208z^3 + 0.871z^4 - 0.988z^5 + z^6$
	b		AR(6)	$Q_1(z) = 1$ $P_1(z) = 1.432 - 1.462z + 1.645z^2 - 1.660z^3 + 1.279z^4 - 1.129z^5 + z^6$
	c (dotted)		ARMA(6,1)	$Q_2(z) = -0.879 + 0.485z$ $P_2(z) = 1.363 - 1.720z + 1.867z^2 - 1.917z^3 + 1.442z^4 - 1.133z^5 + z^6$
	c (solid)		ARMA(6,1)	$Q_2(z) = 0.934 + 0.649z$ $P_2(z) = 1.520 - 1.133z + 1.361z^2 - 1.333z^3 + 1.072z^4 - 1.124z^5 + z^6$

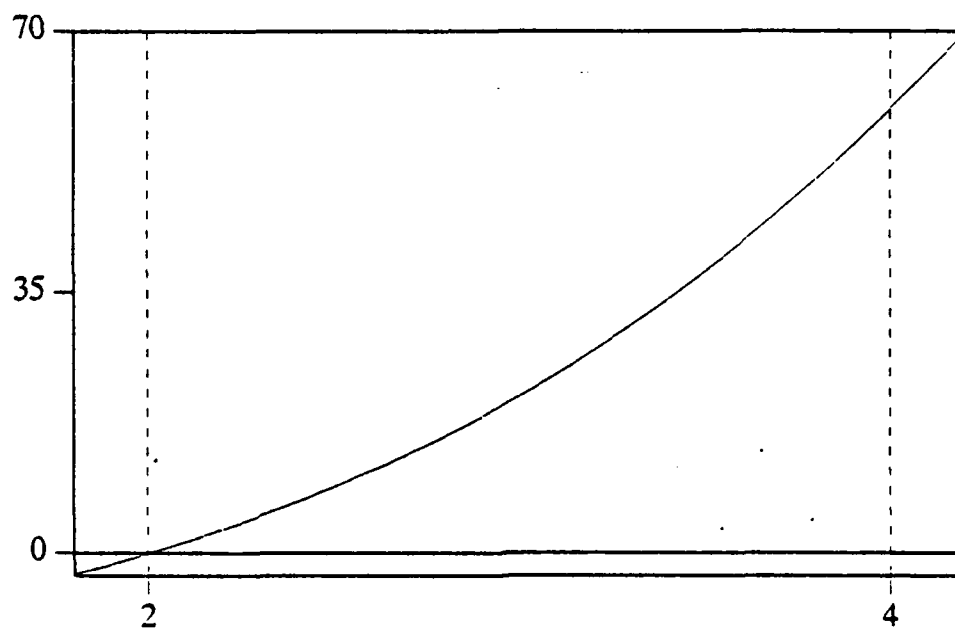


Fig.7 Positivity of $A_0(\beta)$ for $2 < \beta < 4$ (see (B.5)).